Pleistocene uplift, climate and morphological segmentation of the northern Chile coasts (24°S-32°S): Insights from cosmogenic 10Be dating of paleoshorelines

Joseph Martinod, Vincent Regard, Rodrigo Riquelme, German Aguilar, Benjamin Guillaume, Sebastien Carretier, Joaquin Alejandro Cortes Aranda, Laettitia Léanni, Gérard Hérail

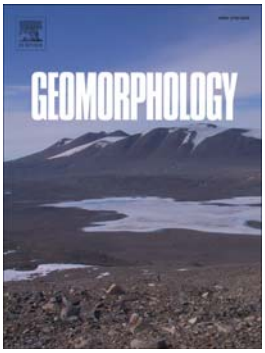

Pleistocene uplift, climate and morphological segmentation of the northern Chile coasts (24S-32S): Insights from cosmogenic ^{10}Be dating of paleoshorelines

Joseph Martinod, Vincent Regard, Rodrigo Riquelme, German Aguilar, Benjamin Guillaume, Sébastien Carretier, Joaquin Cortes, Laetitia Leanni, Gérard Hérail

PII: S0169-555X(16)30832-7
DOI: doi: 10.1016/j.geomorph.2016.09.010
Reference: GEOMOR 5757

To appear in: *Geomorphology*

Received date: 4 November 2015
Revised date: 23 August 2016
Accepted date: 6 September 2016

Please cite this article as: Martinod, Joseph, Regard, Vincent, Riquelme, Rodrigo, Aguilar, German, Guillaume, Benjamin, Carretier, Sébastien, Cortes, Joaquin, Leanni, Laetitia, Hérail, Gérard, Pleistocene uplift, climate and morphological segmentation of the northern Chile coasts (24S-32S): Insights from cosmogenic ^{10}Be dating of paleoshorelines, *Geomorphology* (2016), doi: 10.1016/j.geomorph.2016.09.010

Pleistocene uplift, climate and morphological segmentation of the Northern Chile coasts (24°S-32°S): insights from cosmogenic ^{10}Be dating of paleoshorelines.

Joseph Martinod [a,*], Vincent Regard [b], Rodrigo Riquelme [c], German Aguilar [d], Benjamin Guillaume [e], Sébastien Carretier [b], Joaquin Cortes [a,f], Laetitia Leanni [g], Gérard Hérail [b]

[a] ISTerre, Université de Savoie, CNRS-IRD, 73376 Le Bourget du Lac cedex, France
[b] Géosciences Environnement Toulouse, Université de Toulouse, CNRS-IRD, 14 avenue E. Belin, 31400 Toulouse, France
[c] Departamento de Ciencias de la Tierra, Universidad Católica del Norte, Avenida Angamos, Antofagasta, Chile
[d] Advanced Mining Technology Center, Universidad de Chile, Avenida Beauchef 850, Santiago, Chile
[e] Géosciences Rennes, Université de Rennes, CNRS, Campus de Beaulieu, 35042 Rennes cedex, France
[f] Departamento de ciencias de la Tierra, Universidad de Concepción, Chile
[g] Université Aix-Marseille, CNRS-IRD-Collège de France, UM34 CEREGE, BP 80, 13545 Aix-en-Provence Cedex 4, France

Abstract:

We present new cosmogenic (^{10}Be) exposure ages obtained on Pleistocene marine abrasion shore terraces of Northern Chile between 24°S and 32°S in order to evaluate the temporal and spatial variability of uplift rates along the coastal forearc. Both the dispersion of cosmogenic concentrations in samples from the same terrace and data obtained in vertical profiles show that onshore erosion rates, following emergence of paleoshorelines, approached 1m/Myr. Therefore, minimum ages calculated without considering onshore erosion may be largely underestimated for Middle Pleistocene terraces. The elevation of the last interglacial (MIS-5) paleoshoreline is generally between 25 and 45 m amsl, suggesting that the entire coast of the study area has been uplifting during the Upper Pleistocene at rates approaching 0.3 mm/yr. Available ages for Middle Pleistocene terraces suggest similar uplift rates, except in the Altos de Talinay area where uplift may have been accelerated by the activity of the Puerto Aldea Fault. The maximum elevation of Pleistocene paleoshorelines is generally close to 250 m and there is no higher older Neogene marine sediment, which implies that uplift accelerated during the Pleistocene following a period of coastal stability or subsidence. We observe that the coastal morphology largely depends on the latitudinal climatic

variability. North of 26.75°S, the coast is characterized by the presence of a high scarp associated with small and poorly preserved paleoshorelines at its foot. The existence of the coastal scarp in the northern part of the study area is permitted by the hyper-arid climate of the Atacama Desert. This particular morphology may explain why paleoshorelines evidencing coastal uplift are poorly preserved between 26.75°S and 24°S despite Upper Pleistocene uplift rates being comparable with those prevailing in the southern part of the study area.

Keywords: Andes, Uplift, cosmogenic nuclide, Paleoshores, Tectonics, Climate

1. Introduction

Many authors, following Darwin (1846), noted that most of the Pacific coasts of South America are uplifting. Brüggen (1950) and Fuenzalida et al. (1965) reported the presence of several marine terraces, partly cut in bedrock and partly filled or veneered with clastic materials along most of the Chilean coasts, particularly between 26°S and 40°S. They observed that the elevation of the highest terraces generally exceeds 150 m above mean sea level (m amsl).

The analysis of the Norte Chico coastal morphology and associated continental and marine deposits evidences periods of coastal uplift alternating with periods of subsidence during Tertiary times (Le Roux et al., 2005). In the Tongoy area (~30°S), for instance, Paskoff (1970) describes a period of subsidence marked by the deposit of the Neogene Coquimbo marine formation. He shows that this episode of subsidence followed a period of coastal uplift during which the paleo Limari River had excavated a deep valley, today preserved 500 m below sea level. Although the particular geological evolution of this area has been affected by fault activity, the same succession of periods of uplift interrupted by episodes of subsidence is registered by geological markers in many places of the Norte Chico coastal area. For instance, in the Caldera region (27°S), continental deposits overlain by Miocene marine sediment fill valleys carved in the Paleozoic and Mesozoic basement (Marquardt, 1999; Marquardt et al., 2004).

An active margin coastal area being subject to tectonic uplift or subsidence is not surprising. The question of how subduction drives forearc vertical motions, however, is not clear, and several processes may act together to change the dynamics of the coastal area (e.g., Regalla et al., 2013; Henry et al., 2014; Martinod et al., 2016). In order to constrain the causes of observed motions, it is important to quantify and date the coastal morphological evolution. Scientific questions relative to this issue are listed as follows. When did the present-day coastal uplift begin? Did it occur at constant speed or during short pulses? How does its speed vary laterally? Do periods of uplift and subsidence

correlate everywhere along the Chilean coasts, or are they instead controlled by local tectonic settings?

Answers to the aforementioned questions require dating the beginning of the present-day episode of coastal uplift in Northern Chile. Considering published data, Regard et al. (2010) estimate the onset of coastal uplift in Northern Chile and Southern Peru, looking at the elevation of the highest preserved shoreline and supposing that the vertical velocity remained constant since the beginning of uplift. They propose that coastal uplift started in most sectors of Pacific coasts of the Central Andes during the Middle Pleistocene. In many sites however, the uplift velocity is only constrained by a single age, and there is no information on its temporal variability. Moreover, the constant uplift velocity hypothesis adopted by Regard et al. (2010) conflicts with results obtained by Saillard et al. (2009) in the Altos de Talinay area (~30.5°S). Indeed, data presented by Saillard et al. (2009) suggest that Altos de Talinay have been affected by a pulse of very rapid uplift culminating at 1.2 mm/yr between MIS-9 and MIS-7, preceding a severe decrease of the vertical velocity close to 0.2 mm/yr since MIS-5. It implies that the Pleistocene history of coastal uplift may have been much more complex than supposed by Regard et al. (2010) and, in turn, raises the question of how the geodynamic processes operating in the area may explain highly variable uplift rates.

The spatial variability of coastal uplift in the study area is also disputed. Between 32°S and 26°S ('Norte Chico' region) raised shoreline markers are almost continuously preserved above the present-day coastline (e.g., Brüggen, 1950; Paskoff, 1970), whereas between 24°S and 26 °S ('Norte Grande') the coast is marked by the presence of a high scarp whose elevation approaches 1000 m, and below which terraces or other structures marking the position of ancient seashores are generally absent (see below). In some places north of Tal-Tal (25.4°S), the ocean is actively eroding the scarp. Does the scarp mark a different tectonic evolution and a different uplift velocity north of 26°S?

In the following, we present new cosmogenic data (^{10}Be) to date Pleistocene shorelines in Chile between 24°S and 32°S. We dated terraces in places where no ages where available, in order to look

at the spatial variability of uplift rates. On the other hand, we also dated new paleoshorelines in sites where some terraces had already been dated, in order to evaluate the Pleistocene temporal variability of uplift rates. We confirm that uplift has been active everywhere in the study area during the Middle and Upper Pleistocene. Finally, we show that the morphological signature of coastal uplift in the study area, and particularly the preservation of paleoshorelines, largely depends on climate. Paradoxically, we observe that paleoshorelines are better preserved in the semi-arid Norte Chico than in the hyper-arid Atacama Desert because the coastal cliff, whose preservation is permitted by the hyper-arid climate of Atacama, restrains the formation of wide shore platforms.

2. Coastal morphology of the Norte Chico region, between 24° and 32°S

Both erosional and depositional paleoshores are present in the study area. Erosional paleoshores often consist in staircase marine terraces directly cut in bedrock (abrasion shore platforms). Their formation is related to sea-level highstands associated to the Quaternary glacial/interglacial cycles (e.g., Chapell, 1974; Lajoie, 1986; Pedoja et al., 2014). During sea-level highstands that correlate to odd-numbered Marine Isotopic Stages (MIS), wave action erodes rocky coasts. It results in the appearance of a cliff located above a planar shore platform gently inclined towards the sea. The shoreline angle at the base of the cliff marks the maximum elevation of the ocean during the highstand (e.g., Lajoie, 1986; Jara-Munoz et al., 2016). This erosional surface is abandoned when the sea level falls. If the coast is uplifting, the shore platform is not reoccupied by the ocean, and the bedrock surface morphology is only weakly modified by continental erosion in the semi-arid to hyper-arid environment of Northern Chile. In many places of Northern Chile, the coastal fringe eroded by the ocean corresponds to a ‘Rasa’, i.e. a polygenic surface in which intermediate shoreline angles marking different highstand levels are difficult to observe (Guilcher, 1974; Regard et al., 2010).

Depositional paleoshores result in terraces where marine deposits accumulated. They are generally covered by beach-ridges, and their presence in Northern Chile is generally restricted to bays where the energy of waves is lower (Saillard et al., 2012).

The morphology of the coast varies significantly depending on the bedrock lithology, the continental slope close to the present-day shoreline, and the considered latitude. We describe below, from north to south, the morphology of this segment of the Chilean Coast. See Fig. 1 for the geographical location of sites cited in the text.

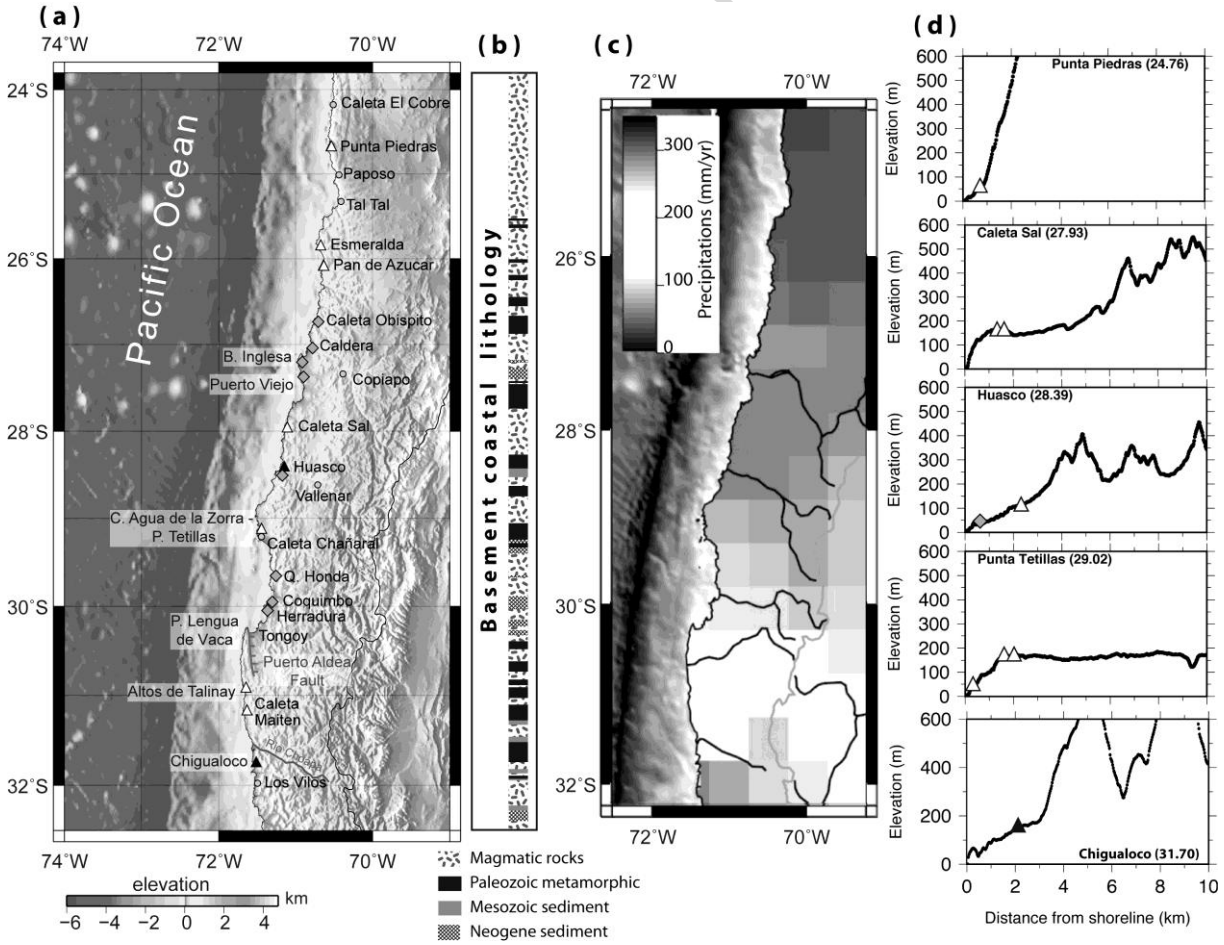

Figure 1: *(a) Location of dated marine paleoshorelines and other sites cited in the text. Empty triangles: ^{10}Be data on surface samples; filled triangles: ^{10}Be data in vertical profiles; diamonds: other dating methods; (b) Basement lithology along the coast; (c) Average annual precipitations between 1960 and 1990 (after Willmott & Matsuura, 2001); (d) Topographic profiles perpendicular to the coast.*

The coast of the northern part of the study area between Caleta El Cobre (24°S) and Caleta Obispito (26.75°S) is particularly steep (Fig. 1). In many segments, it is marked by the presence of a scarp built in Mesozoic volcanic and plutonic rocks whose elevation approaches 1000 m. The distance between the scarp and the present-day coastline is generally ~1 km. Most of the fringe between the coast and the scarp is composed by a single rasa, whose inner edge elevation is often lower than 100 m amsl, and no remnants of Pleistocene marine erosion are preserved at higher elevations. In some places, especially north of Tal-Tal (25.4°S), the coastal rasa totally disappears and the ocean is actively eroding the scarp. In this northern segment (24°S-25.4°S), the rasa at the base of the coastal scarp corresponds to a rough surface in which many ancient seastacks have been preserved, often covered by thick caps of debris fallen from the scarp. In many places, the bedrock is not visible beneath the scarp and the ocean is actively eroding the cap of fallen debris. Very few flat terraces containing marine deposits between sea stacks are preserved north of Tal-Tal. The larger ones are located close to Planta Paposo (25.1°S) and above Punta Piedras (24.75°S) (Fig. 2). The marine terrace located above Punta Piedras is only ~150 m wide per ~300 m long.

Figure 2: *View from the South of the Punta Piedras terrace beneath the coastal scarp (24.75°S).*

The coastal segment located south of Caleta Obispito (26.75°S), in contrast, presents a gentle topography. Between Caleta Obispito and Caleta Sal (27.9°S), Pleistocene paleoshorelines often lie above Neogene marine sediment pertaining to the Bahia Inglesa Formation. Numerous paleoshorelines marked by the occurrence of beach ridges are visible between the present-day coastline and ~220 m amsl (Marquardt, 1999; Marquardt et al., 2004).

Between 27.9°S and 28.8°S (Caleta Sarco), Neogene deposits disappear and Pleistocene terraces are generally built above Paleozoic metamorphic series and Mesozoic intrusives. Large parts of the coastal fringe affected by marine erosion are covered by aeolian deposits, masking the morphology inherited from marine erosion. The width of the coastal fringe affected by Pleistocene marine erosion is roughly 2 km. In Huasco (28.5°S), Cooke (1964) and Fuenzalida et al. (1965) note the presence of several narrow lower terraces. Above lower terraces, the coastal fringe consists of a large upper rasa, whose inner limit is between 130 and 220 m amsl.

The coastal area located between 28.8°S (Caleta Sarco) and 29.35°S (Choros Bajo) corresponds to a wide low elevation area. The basement consists in Paleozoic metamorphic series, Jurassic plutons, covered in some places by Neogene deposits of the Coquimbo Formation. Pleistocene marine paleoshorelines are preserved as far as 15 km onshore. Paleoshores consist either of abrasion terraces, or of beach ridges deposited above surfaces gently inclined toward the ocean. Lower terraces are narrow, they contain many preserved seastacks, and in many places their shoreline angle and the transition with the upper terrace is difficult to observe. In Caleta Agua de la Zorra, 15 km north of Caleta Chañaral, narrow marine terraces whose inner edge elevations are located 34, 54 and 74 m amsl are preserved. Shoreline angles of two higher terraces 92 and 110 m amsl are clearly visible 10 km to the south, close to Punta Tetillas. All these narrow terraces contain many preserved seastacks, and their morphology contrasts markedly with that of the upper marine terrace. The upper terrace, indeed, is several km-wide, flat and polished, and few seastacks have been preserved by marine erosion on this level (Fig. 3).

Between 29.35°S and 29.8°S, Neogene deposits disappear and marine terraces are again built in Mesozoic volcanic and plutonic rocks, except in Quebrada Honda (29.6°S) where the Neogene Coquimbo Formation locally outcrops. Within Mesozoic rocks, marine erosion resulted in the appearance of a ~2 km-wide rasa. The inner edge of the rasa is generally 200 m amsl. Its surface is generally rough, including many ancient seastacks between 1 and 100 m long, and it is difficult to distinguish terraces in this geomorphological unit.

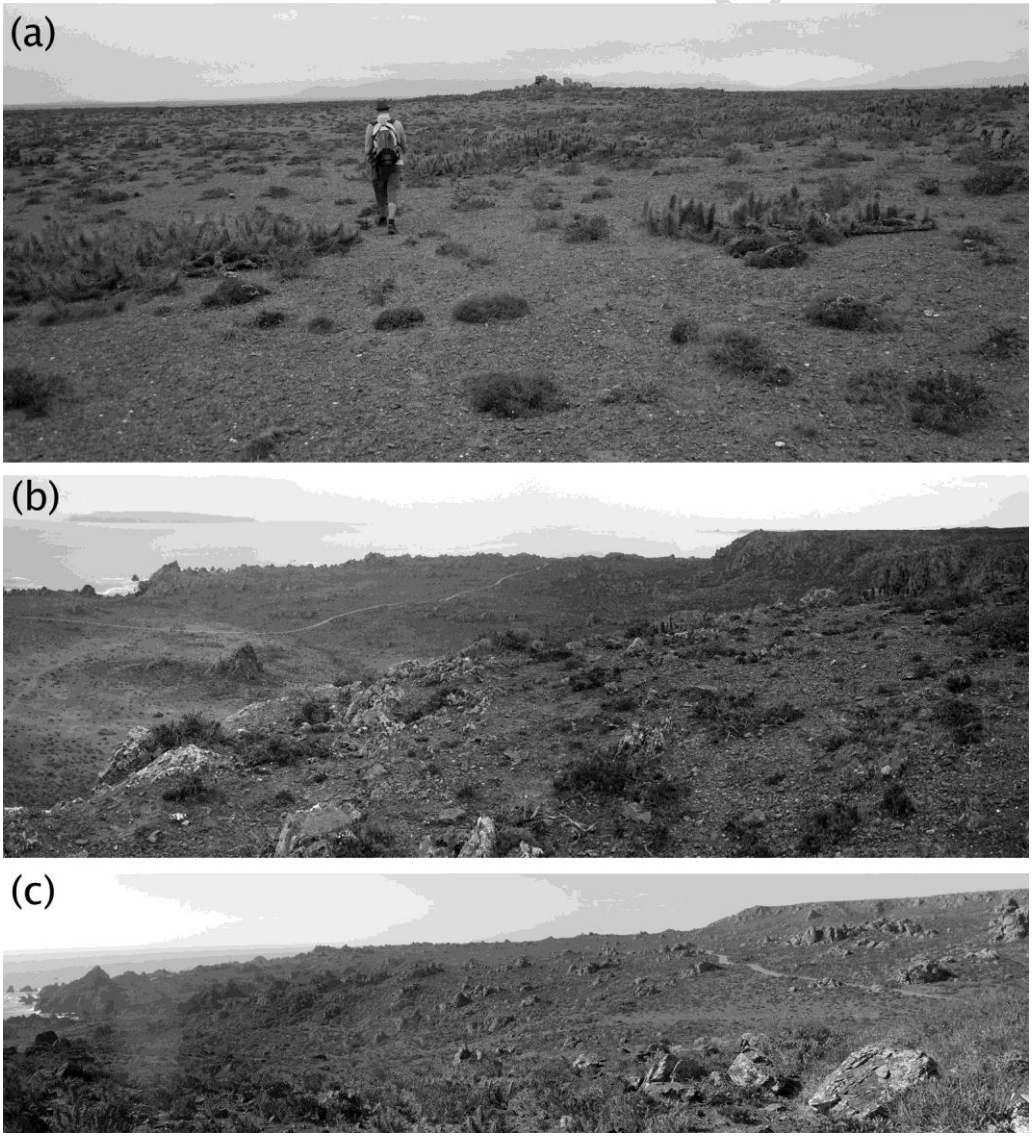

Figure 3: *Contrasted morphology of the upper and lower terraces in Punta Tetillas (29°S). (a) The upper terrace is several km wide, and it has been almost completely polished by marine erosion. Only rare seastacks have been preserved. (b) View taken from the upper surface towards the*

ocean and (c) photo taken from one of the lower terraces. Lower terraces are rough, narrow, and shoreline angles marking different highstand levels may be difficult to observe.

Between 29.8°S and 30.3°S, the coastline is composed of several bays that are, from north to south, the Coquimbo, Herradura, Guanaqueros and Tongoy bays (Fig. 1). These bays are marked by depositional paleoshores whose morphology is dominated by numerous beach ridges deposited above Neogene marine sediments pertaining to the Coquimbo Formation (Brüggen, 1929). In Tongoy Bay, three levels of marine terraces are preserved (Paskoff, 1970), while four major terrace levels had already been recognized in the Coquimbo Bay by 19th century geologists (Darwin, 1846; Domeyko, 1848). The maximum elevation of Quaternary marine deposits is approximately 160 m amsl.

The SE boundary of Tongoy Bay corresponds to the Puerto Aldea Fault (Fig. 1), whose Pleistocene activity has been noted by Paskoff (1970), Ota et al. (1995) and Saillard et al. (2012). The fault azimuth is approximately N-S, and it accommodates the uplift of the western block (Punta Lengua de Vaca). The morphology of the coastal segment located between Punta Lengua de Vaca and Los Vilos (32°S) is fully described in Paskoff (1970), Ota et al. (1995) and Saillard et al. (2009). Abrasion surfaces built by oceanic erosion are particularly well preserved along this 150 km-long coastal segment, and authors distinguish four main marine terraces. The two highest platforms (denominated TI and TII in Ota et al. (1995)) are much larger than underlying terraces. TI and TII consist in large surfaces gently inclined towards the ocean. Their width is generally greater than 5 km, and their maximum elevation is approximately 500 m and 200 m, respectively. Lower terraces, in contrast, (TIII and TIV following Ota et al. (1995)) correspond to rough terraces in which many sea stacks are preserved, and their width is always less than 1 km. The maximum elevation of TIII is approximately 50 to 60 m, and that of TIV is ~25 m amsl. In the coastal segment between Punta Lengua de Vaca and Los Vilos, highest surfaces (TI and TII) are cut by faults whose azimuth is generally close to N165°, and that accommodate the uplift of the western block without any significant strike-slip motion (Ota et al., 1995; Saillard et al., 2010). The largest of these faults crosses

the Quebrada del Teniente valley, 17 km north of Caleta Maiten. Ota et al. (1995) report that the El Teniente Fault vertical offset through the high surface is approximately 50 m. They also note that the El Teniente Fault and other similar structures are apparently inactive, since lower marine terraces below 50 m amsl are not deformed.

To sum up, there is a sharp contrast in the coastal morphology north and south 26.75°S. In the northern part of the study area, the coastal fringe is narrower than ~1 km, its inner edge often corresponds to a very high scarp whose elevation approaches 1000 m, and paleoshorelines marking coastal uplift are poorly preserved. In contrast, paleoshorelines have a continuous longitudinal expression south of 26.75°S. This different morphology is not explained by lithology, since similar magmatic series constitute the larger proportion of coastal segments both north and south of 26.75°S (Fig. 1b). Finally, we also observe that higher preserved Pleistocene terraces are generally smoother and wider than lower terraces.

3. Previously published ages and sampling strategy

Fuenzalida et al. (1965) noted that paleontological data do not help in accurately dating shoreline changes. They show, however, that the highest raised shorelines are not older than the Pleistocene or Pliocene**.** Between Caleta Sal and Caldera, Marquardt (1999), Ortlieb et al. (2003) and Marquardt et al. (2004) describe a terrace whose elevation varies between 135 and 160 m amsl, containing warm water mollusks that live today north of 6°S along South American coasts. Ortlieb et al. (2003) proposed that this warm water fauna, also called TAMA (Thermally Anomalous Molluscan Assemblage), expanded southward when the intensity of the cold Humboldt current diminished, during MIS-11 (400 kyrs ago). However, U-Th data obtained by Leonard et al. (1994) in Morro Copiapo (27.2°S) in a terrace containing TAMA fauna suggest that warm water mollusks deposited during an older interglacial period (MIS-13 or MIS-15, Marquardt et al., 2004). Moreover, north of the study area, in the Mejillones Peninsula (23°S), Cortes (2012) shows that at least two levels

contain warm water assemblages. Thus we consider that although TAMA deposits may help in correlating terraces, their age is not constrained enough to give precise information on the coastal uplift.

Paleoshorelines in the study area have been dated using different techniques. The U/Th method has been employed on marine shells by Radtke (1987a; 1987b; 1989), Leonard et al. (1994) and Saillard et al. (2012). Other methods applied on shells consist in mollusk aminostratigraphy and Electron Spin Resonance (ESR) ages (Leonard & Wehmiller, 1992). All these methods are appropriate to date shores from the more recent interglacial periods. In contrast, they do not permit accurate dating of shores older than ~400 kyr (MIS-11). In fact, most of the ages obtained using these techniques correspond to the lower paleoshorelines that mark the last or penultimate interglacial period (MIS-5 or MIS-7), and little information is available concerning older seashores.

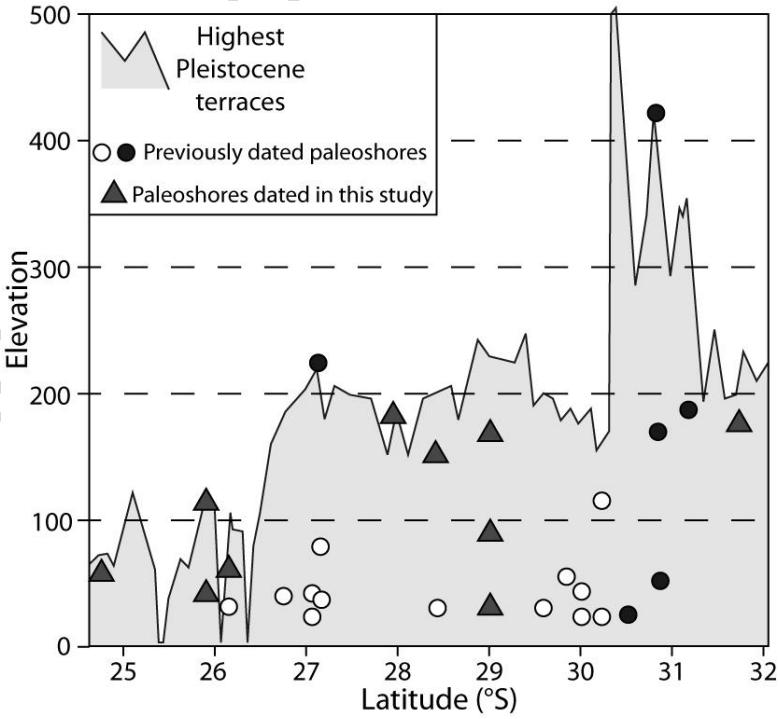

Figure 4: *Latitude vs. elevation of dated paleoshorelines. Circles correspond to paleoshorelines dated in previous studies, filled circles corresponding to paleoshorelines dated using cosmogenic isotopes whose ages are discussed again in this paper. Triangles correspond to paleoshorelines sampled and dated in this work.*

More recently, cosmogenic isotopes have also been used to date Quaternary paleoshorelines in Northern Chile (Quezada et al., 2007; Saillard et al., 2009; Rodriguez et al., 2013). Quezada et al. (2007) measured ^{21}Ne concentrations in pebbles collected in a terrace above Caldera (27°S). However, they note that concentrations differ significantly between pebbles collected in the same paleoshoreline, suggesting that some of them contain large amounts of inherited cosmogenic isotopes. The problem of inherited concentration is avoided if directly sampling bedrock outcrops. In many terraces in Northern Chile, the ocean removed most of the eroded material, and the bedrock either directly outcrops or is covered by a very thin (<1 m) layer containing rounded pebbles, sand and shells. Measuring cosmogenic isotopes concentrations in bedrock samples from these terraces should indicate the timing of emersion of the terrace, or a minimum age in case the erosion that followed emersion cannot be neglected. Saillard et al. (2009) measured ^{10}Be concentrations as large as 2.9×10^6 atoms/g in quartz samples collected 240 m amsl in Altos de Talinay (30.9°S), evidencing that the erosion posterior to the formation of this paleoshoreline has been slower than 1 m/Myr there. These authors remark that samples collected on the same terrace have comparable ^{10}Be concentrations. They also observe that ages estimated from cosmogenic isotope concentrations and supposing that the erosion has been negligible following the emersion of the terrace (minimum ages) correspond to sea-level highstand periods. Thus, they conclude that post-emergence erosion did not affect the cosmogenic isotope concentrations in the samples they collected, and that minimum ages calculated neglecting erosion processes give a good estimation of the real seashore age even for terraces that date from the beginning of the Middle Pleistocene (MIS-19, ~690 kyr). Indeed, they note that in the Central Depression and Precordillera of Northern Chile, Nishiizumi et al. (2005) and Kober et al. (2007) report erosion velocities generally smaller than 1 m/Myr, and often as small as 0.1 m/Myr. Nevertheless, Saillard et al. (2009) acknowledge that samples they analyzed were collected in small areas (within a radius of ~6 m) within each terrace, which may also explain the small variability

of measured concentrations. Moreover, we note that erosion rates as small as 1 m/Myr significantly decrease cosmogenic isotope concentrations in Middle Pleistocene surfaces.

Except in Bahia Inglesa (~27°S) and Tongoy-Altos de Talinay (30.5°S - 31°S), only one terrace has been dated per site, which does not permit evaluating the temporal variability of uplift. In Bahia Inglesa, Marquardt et al. (2004) propose that the uplift velocity remained close to 0.32 mm/yr since MIS-11. Quezada et al. (2007) dated older (860 kyr-old) paleoshorelines in the same sector. The average uplift velocity they calculate is slightly smaller than that proposed by Marquardt et al. (2004), and they note that this difference may evidence a moderate acceleration of the vertical coastal velocity during the second half of the Middle Pleistocene. In contrast, in the Altos de Talinay area (~30.5°S), data presented by Saillard et al. (2009) suggest highly variable uplift rates during the Middle and Upper Pleistocene (see Introduction).

Our sampling strategy considered evaluating both the spatial and temporal variability of uplift rates during the Middle and Upper Pleistocene in the study region. We sampled preferentially basement in abrasion shore terraces, considering that post-emergence erosion rates are small enough to permit a precise dating of surfaces whose age may be as old as the beginning of Middle Pleistocene, which was suggested by Saillard et al. (2009). We did not sample terraces covered by post-emergence deposits such as colluviums coming from the overlying cliff, or aeolian deposit that are frequent in some sectors of the coast. We also avoided sampling terraces whose inner edge elevation is not easy to determine. We estimated samples and the corresponding shoreline angle elevations using an altimeter calibrated at sea level whose precision is $\pm$ 5 m. When possible, we dated high elevation paleoshorelines in areas where low terraces had already been dated by previous authors, to obtain information on the temporal variability of uplift. We also sampled areas of the study region where no data were available such as Caleta Chañaral (29°S) and the coast north of Pan de Azucar (26.1°S).

In the following, we present and discuss measured cosmogenic isotope concentrations. We observe that erosion rates are not as small as assumed by Saillard et al. (2009). Indeed, the variability of values measured in bedrock samples for a same paleoshoreline shows that the erosion rate may largely influence ^{10}Be concentrations, particularly when looking at several hundred kyr-old markers. We also present ^{10}Be concentrations in two vertical profiles confirming that post-emergence erosion of marine terraces cannot be neglected.

4. Results: Cosmogenic ^{10}Be concentrations, erosion rates and age of paleoshorelines

4.1. Vertical profiles

Bedrock samples have been collected in two vertical profiles. Cosmogenic isotope production attenuates rapidly with depth in the basement and becomes negligible 10 m beneath the surface (Braucher et al., 2003; 2011; Nishiizumi et al., 2007). With preserved paleocliffs being generally higher than 10 m, we assume that bedrock samples did not accumulate cosmogenic isotopes prior to terraces formation. In Chigualoco (31.7°S), the highest paleocliff is located onshore, ~3 km from the present-day coastline, and the elevation of the shoreline angle at the base of the cliff is approximately 180 m amsl. The profile is drilled 146 m amsl in an altered granitoid, in the widest and highest terrace. The basement is covered by a ~30 cm-thick soil. ^{10}Be concentrations are given in Table 1 and presented in Fig. 5. The shape of concentration profiles in cosmogenic isotopes depends on the ratio between the isotopic production by spallation and that resulting from muons (e.g., Braucher et al., 2003). Production by muons is minor close to the surface, but becomes predominant at depth since muons penetrate deeper. This production, however, is poorly known (see discussion in Braucher et al., 2011). Considering production values proposed by the Cronus-Earth web calculator (Balco et al., 2008), ^{10}Be concentrations vs. depth in Chigualoco suggest that the surface is older than 2 Myrs and at steady-state, with an erosion rate between 1.5 and 2.0 m/Myr. It is not possible to explain the observed profile considering the production rates proposed by Braucher et al. (2011),

except if we assume that rocks at depth contained some inherited cosmogenic isotopes, which is unlikely in basement rocks. The best fit of the profile using Braucher et al. (2011) production rates is shown in Fig. 5. This fit also suggests the surface to be at steady-state, but proposes a smaller erosion rate (close to 1.1 m/Myr).

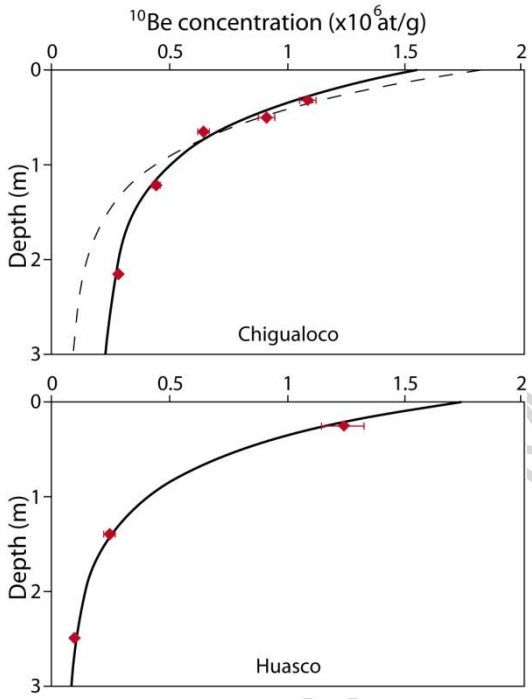

Figure 5: *^{10}Be concentrations along vertical profiles sampled in marine terraces in Chigualoco and Huasco. The solid and dashed lines in the Chigualoco profile represent the best fit obtained using the cosmogenic production rates proposed by Balco et al. (2008) and by Braucher et al. (2011), respectively.*

Another vertical profile has been sampled close to Huasco, 110 m amsl, in the higher and wider terrace whose shoreline elevation is 155 m amsl. Depending on the adopted ^{10}Be muonic production rate, the profile fits with a terrace that was carved between 0.5 and 2.5 Myr ago, and has been eroding between 0 and 1 m/Myr (Fig. 5).

4.2. Surface samples, erosion rates and ages

^{10}Be concentrations have been measured in 26 new surface samples, collected in 8 terraces from 5 sites between 24°S and 32°S (Table 1). Cosmogenic concentrations in bedrock samples depend on both the age of the surface and erosion rate. We generally sampled bedrock directly outcropping on marine terraces, and sometimes quartz clasts and rounded pebbles or gravels collected within a thin regolith covering the surfaces. Rounded gravels and pebbles cannot have been produced onshore in these environments. They were shaped by marine erosion and are often found in a thin and discontinuous sedimentary layer covering terraces, mixed with sand and marine shells. Thus, they may contain inherited cosmogenic isotopes acquired before the formation of the terrace on which they lie. Quartz clasts are collected close to eroding seastacks or on very flat surfaces, and we assume they either come from bedrock erosion close to the sampling location, or from rounded pebbles that have been fragmented by physical weathering (insolation weathering). Different samples from the same terrace were generally collected at several tens of meters of distance between each other, in order to analyze the variation in superficial cosmogenic isotope concentrations within terraces.

^{10}Be concentrations in samples from the same terrace often present significant variations, as for instance in the highest terrace in Caleta Chañaral (Table 1). This result differs from that obtained by Saillard et al. (2009). ^{10}Be concentrations in bedrock samples are often larger than those measured in clasts and rounded gravels, despite clasts and rounded gravels may contain inherited cosmogenic isotopes. We conclude that in these surfaces, the erosion rate significantly affects the concentration in cosmogenic isotopes. Erosion is more intense where soft sediment covers the surface than in bedrock, which may explain larger cosmogenic concentrations in bedrock samples. In Caleta Chañaral, the minimum ^{10}Be concentration measured on the highest surface (1.44×10^6 at/g) shows that the erosion rate remained smaller than 1.4 m/Myr. However, this value is far from negligible when considering terraces whose formation is several hundreds of kyrs old, and minimum ages calculated assuming no erosion may be much smaller than the real age of formation of the terrace. In Table 2, we present ages calculated for different erosion rates between 0 and 1.5 m/Myr for the

surface samples we collected, using the Cronus-Earth web calculator (Balco et al., 2008). Table 2 also indicates ages calculated from ^{10}Be concentrations published in Saillard et al. (2009) and in Rodriguez et al. (2013), for different possible erosion rates. It shows that taking into account erosion rates largely modifies calculated ages for ancient terraces. For instance, surface sample ^{10}Be concentrations in 400 kyr-old (MIS-11) terraces without onshore erosion are similar to concentrations in 670 kyr-old (MIS-17) terraces whose erosion rate is 1 m/Myr. For younger terraces that formed during the last or penultimate interglacial period (MIS-5 or MIS-7), the dependence of calculated ages on erosion rates is much smaller. For instance, ^{10}Be concentrations in MIS-5e (124 kyr-old) terraces only differ by less than 10% when the erosion velocity changes from 0 to 1 m/Myr, whereas the corresponding difference is 34% and 60% in MIS-11 and MIS-17 terraces, respectively.

5. Discussion:

5.1. Assignment of paleoshorelines to sea-level highstands using ^{10}Be data

We observe that terraces whose elevation is between 100 and 200 m amsl are older than 400 kyr (MIS-11), meaning that the uplift rate has everywhere been smaller than 0.5 mm/yr. Most authors that calculated uplift velocities in the study area based on other dating techniques also concluded that uplift velocities since MIS-5 and during the Middle Pleistocene remained lower than 0.5 mm/yr (e.g., Leonard & Wehmiller, 1992; Marquardt et al., 2004; Quezada et al., 2007). Worldwide preserved paleoshoreline sequences generally contain shores built during MIS-5, 7, 9 and 11 that are 124 kyr, 210 kyr, 320 kyr and 400 kyr-old, respectively (Siddall et al., 2006; Pedoja et al., 2014). Indeed, sea level during these interglacial periods was close to the present-day one, and related paleoshorelines are now emerged even if the coastal uplift rate has been small. Shore terraces may also form during sea-level lowstands (e.g., MIS-2). They correspond to drowned terraces, and their morphology is modified during later interstadial oscillations or highstands if the coast is slowly uplifting. Thus, shores forming during sea-level lowstands are generally destroyed by marine erosion

except if the coastal uplift has been larger than the subsequent sea-level rise, which requires uplift rates greater than several mm/yr (Caputo, 2007). Shores formed during interstadial oscillations (e.g., MIS-3) when sea level was several tens of meters lower than today are only preserved onshore if the uplift rate has been rapid. For instance, uplift rates larger than 1.2 mm/yr or 1.5 mm/yr are necessary to preserve shores related to MIS-3 (Pedoja et al., 2014; Jara-Munoz and Melnick, 2015). Then, the moderate uplift rates observed in the study area suggest that preserved paleoshorelines in Northern Chile were formed during sea-level highstands, as discussed in Saillard et al. (2010).

Table 2 shows that cosmogenic isotope concentrations do not permit precise assigning of paleoshorelines to sea-level highstands for terraces higher than 100 m amsl. Indeed, we do not constrain onshore erosion whose effect becomes predominant for old surfaces. Sea-level highstand assignments are easier for lower and younger terraces, as explained above. We discuss below the cosmogenic concentrations measured in paleoshore samples, from north to south. We propose, when possible, the assigning of terraces to sea-level highstand periods (see Table 3).

Punta Piedras (24.76°S): We analysed four samples, three of them collected in bedrock and one corresponding to quartz clasts collected between ancient sea-stacks on the terrace. Cosmogenic concentrations in the four samples give coherent ^{10}Be concentrations between 4.8x10^5 and 6.1x10^5 at/g. These concentrations suggest that the Punta Piedras terrace formed during MIS-5e, ~124 kyrs ago (Table 2).

Esmeralda (25.9°S): ^{10}Be concentrations measured in the bedrock 45 m amsl show that marine erosion has been active at this elevation during the last interglacial period. The inner edge of the coastal rasa is generally below 100 m amsl. Above the main rasa, a small terrace located ~115 m amsl, covered by a thin cap of pebbles has been locally preserved. Concentrations in cosmogenic isotopes indicate a minimum age for this latter terrace of 424+/-44 kyrs (Table 2), i.e. that it formed during or before MIS-11.

Pan de Azucar (26.15°S): We sampled ancient sea-stacks between 53 and 64 m amsl. Concentrations in cosmogenic isotopes correspond to minimum ages close to 200 kyrs (except one sample at 282 (+/-32) kyrs), suggesting that sampled seastacks formed during the penultimate glacial period (MIS-7).

Coastal segment between Caleta Obispito (26.75°S) and Huasco (28.4°S): In Caleta Sal, we measured ^{10}Be cosmogenic concentrations both in bedrock and rounded pebbles from the highest terrace, 170 m amsl. Concentrations reach 1.9×10^6 at/g, indicating a minimum age of 460 kyr for the formation of this terrace (Table 2). This value is coherent both with the age obtained by Quezada in Bahia Inglesa, 80 km north of Caleta Sal, on the highest 224 m amsl terrace (~860 kyrs), and with the profile presented above sampled close to Huasco, 50 km to the south. These three data suggest that the highest preserved Pleistocene paleoshoreline in this segment of the coast formed between 500 kyrs and 1 Myr.

Caleta Chañaral (29°S): Close to Punta Tetillas, in two sites 500 m apart, we sampled quartz veins, quartz clasts and rounded quartz pebbles on the surface of the upper terrace, at an elevation of 160 m amsl. Minimum ages deduced from cosmogenic concentrations in bedrock samples are 591 (+/-63) and 404 (+/- 41) kyrs (Table 2). Concentration in cosmogenic isotopes in quartz clasts and rounded pebbles are close or slightly smaller than in quartz veins, suggesting that a very thin cap of sediment has been removed from the surface by continental erosion following the formation of the terrace.

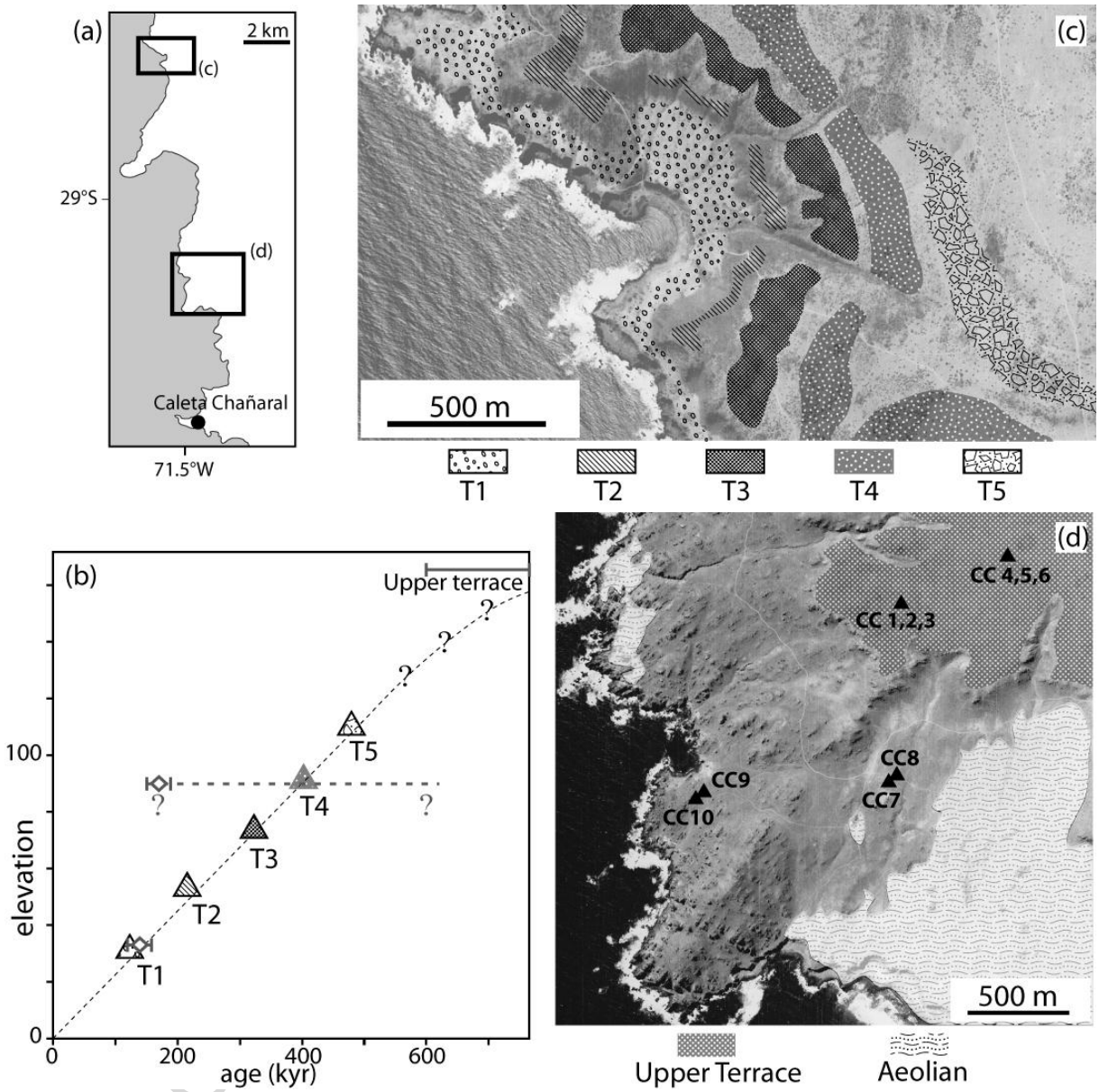

Figure 6: *Map and inner edge elevation of coastal terraces located close to Caleta Chañaral. The location of detailed maps (c) and (d) is given in (a). (b) Assigning terraces to successive odd-numbered isotopic stages (triangles) implies a remarkably constant uplift rate close to 0.25 mm/yr. Minimum ages deduced from ^{10}Be concentrations in samples from Punta Tetillas (empty diamonds) confirm that T1 corresponds to MIS-5, and that the higher 160 m amsl terrace is older than 600 kyrs. See the text for the discussion of ^{10}Be concentrations.*

We also measured ^{10}Be concentrations in four bedrock samples collected at lower elevation, in poorly preserved terraces containing many seastacks. The two samples collected on the terrace whose shoreline angle is ~34 m amsl indicate that this level is 138 ±15 kyrs-old and corresponds to

the last interglacial period (MIS-5) (Table 2). We do not explain the relatively low ^{10}Be concentrations measured in the two samples collected 90 m amsl. They suggest that the terrace whose shoreline angle is 92 m amsl may have formed during MIS-5 or MIS-7. These ages would require a very rapid uplift rate following MIS-7, contrasting with a much smaller uplift rate that may have prevailed between the formation of the large upper terrace and MIS-7. Alternatively, these small concentrations in cosmogenic isotopes may result from sediment that temporarily covered the sampled area. Indeed, aeolian deposits are present only 500 m east of the two samples collected 90 m amsl (Fig. 6d). Then, dunes may have covered them in the past, explaining their low concentration in cosmogenic isotopes, and minimum ages deduced from these concentrations may differ significantly from the age of the terrace.

Another method to estimate the coastal uplift rate is to suppose that the lower terraces observed in Caleta Agua de la Zorra and Punta Tetillas formed during successive Pleistocene highstand periods. If we assume that the 34 m amsl terrace formed during MIS-5e, the following one during MIS-7 and so on, the calculated uplift rate is remarkably constant (~0.25 m/kyr, see Fig. 6 and Table 3). Now, assuming that this uplift rate maintained constant since the final emersion of the uppermost rasa, the upper terrace would be ~700 kyrs-old, which is compatible with cosmogenic data.

Chigualoco - Altos de Talinay coastal segment (31.5°S – 30.2°S)

Saillard et al. (2009) measured ^{10}Be concentrations on the four main platforms. Samples were collected 241 m amsl, 102 m amsl, 30 m amsl and 18 m amsl for TI, TII, TIII and TIV terraces, respectively, and gave minimum exposure ages of 679, 318, 225 and 149 kyrs. Considering that post-emersion erosion has been negligible and does not affect cosmogenic isotope concentrations, Saillard et al. (2009) assigned terraces TI, TII, TIII and TIV to MIS 17, 9, 7, and 5, respectively. These authors also considered that the maximum position reached by the ocean during each of these highstand levels corresponded to the shoreline angle preserved above each sampling point, i.e. that MIS-17, 9, 7 and 5 marine transgressions reached elevations of 425, 170, 55 and 25 m amsl,

respectively. As discussed above, onshore erosion may limit cosmogenic concentrations and result in underestimated ages, particularly for ancient terraces. Cosmogenic concentrations published in Saillard et al. (2009) for terrace TII may result from a terrace formed during MIS-9 in the absence of erosion. Alternatively, it may also correspond to a terrace that formed during MIS-11 and that suffered moderate (1 m/Myr, see Table 2) onshore erosion comparable to that observed in our profiles (e.g., in Chigualoco, see above). Moreover, assigning this terrace to MIS-9 implies that the uplift rate decreased from an exceptionally high value (1.2 mm/yr) between MIS-9 and MIS-7 to much lower values (~0.2 mm/yr) following MIS-7. Saillard et al. (2011) propose that this velocity decrease marked the end of the Quaternary activity of the Puerto Aldea Fault. Assigning terrace TII to MIS-11 would also require a diminution of the Altos de Talinay uplift velocity following MIS-7, but the corresponding uplift rate between MIS-11 and MIS-7 (0.6 mm/yr) would have been in the range of vertical velocities observed elsewhere in Northern Chile.

For the same reasons, we argue it is difficult to assign the Caleta Maiten terrace sampled by Rodriguez et al. (2013) to a precise highstand period, and the cosmogenic data only give a minimum age for this terrace.

5.2. Pleistocene uplift rates in Northern Chile between 24°S and 32°S

Assigning paleoshorelines to sea-level highstands gives information on the uplift that occurred following the emersion of the marker. Apparent uplift rates presented in Table 3 correspond to paleoshoreline elevations divided by their age. Paleoshorelines formed during sea-level highstands when the level of the ocean was close to the present-day sea level (Siddall et al., 2006). Hence, the apparent uplift rate is a good first order estimation of the tectonic uplift velocity. Calculating absolute uplift rates requires knowing the precise sea-level elevation during highstands, which is a controversial issue (e.g., Simms et al., 2016). Table 4 summarizes the age of Middle and Upper Pleistocene highstands and the corresponding sea-level elevations according to Siddall et al. (2006).

Table 3 and Fig. 7 shows minimum and maximum possible absolute uplift rates, calculated considering eustatic variations presented in Table 4.

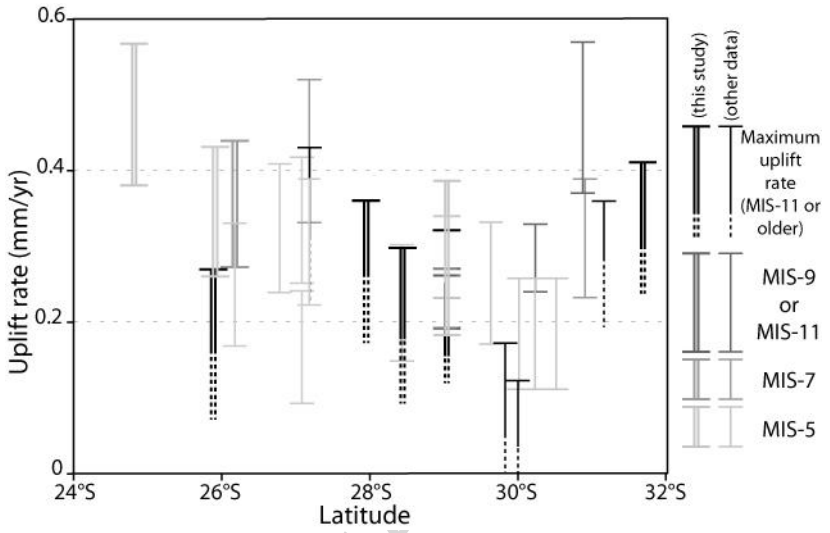

Figure 7: *Absolute uplift rates calculated considering Pleistocene eustatic variations proposed by Siddall et al. (2006) (see Table 3)*

The maximum elevation of terraces formed during the last interglacial period (MIS-5) generally varies between 25 m amsl (Tongoy and Coquimbo) and 45 m amsl (Esmeralda and Caldera) (Table 3). Only one higher terrace located 60 m amsl, in Punta Piedras, has been assigned to MIS-5. These data show that the entire coast of Norte Chico has been uplifting during the upper Pleistocene, with apparent uplift rates generally between 0.18±0.08 and 0.35±0.08 mm/yr (Table 3), with a maximum of 0.48±0.09 mm/yr in Punta Piedras. Data do not show major changes in uplift rate between neighbor points, confirming that no superficial crustal fault deformed the coastal zone during the Upper Pleistocene. In particular, the Puerto Aldea Fault that accommodates the uplift of the Altos de Talinay with respect to Tongoy Bay does not displace MIS-5 paleoshorelines. It shows that this fault remained apparently inactive during the Upper Pleistocene, as already noted by Saillard et al. (2011). We also highlight that this range of uplift rates is a compilation of various methods applied in different geomorphologic features (erosional vs. depositional coasts), and that data obtained using different methods in neighbor points generally indicate comparable uplift rates.

When available, uplift rates calculated considering older paleoshorelines (MIS-7 and MIS-9) are close to those calculated for the Upper Pleistocene (since MIS-5) (Fig. 7). In fact, absolute uplift rates calculated since the penultimate highstand (MIS-7) are generally slightly larger than those calculated considering MIS-5 and MIS-9 paleoshorelines. In Pan de Azucar, Bahia Inglesa, Caleta Chañaral and Altos de Talinay the average absolute uplift rate since MIS-7 is between 0.05 and 0.13 mm/yr higher than that calculated considering MIS-5. In Caleta Chañaral, the average absolute uplift rate since MIS-7 is also 0.08 mm/yr higher than that calculated since MIS-9 and MIS-11. Following Siddall et al. (2006), we assumed that the maximum sea level was -10±5 m amsl during MIS-7. These authors note, however, that this value is debated, some data suggesting that the sea may have risen above the present-day sea level. Then, the systematic bias towards larger MIS-7 absolute uplift rates may simply result from an underestimated elevation of sea level during this highstand.

In many places, the new cosmogenic data obtained in high terraces do not constrain precisely the age of terraces because post-emergence erosion rates cannot be quantified. Only minimum ages, and hence maximum uplift rates, can be calculated. These uplift rates are generally close to those obtained considering lower paleoshorelines, suggesting that uplift rates remained approximately constant during the Middle and Upper Pleistocene, as already proposed for the Bahia Inglesa area by Quezada et al. (2007). The only area in which uplift rates significantly varied since MIS-11 is the Altos de Talinay area, SW of the Puerto Aldea Fault. This has been evidenced by Saillard et al. (2009), even if changes in uplift rates may have been much smoother than proposed by these authors (see discussion above, section 5.1). This change in uplift rates may mark the activity of the Puerto Aldea Fault that may have accommodated the accelerated uplift of the Altos de Talinay area before MIS-7 (Saillard et al., 2011).

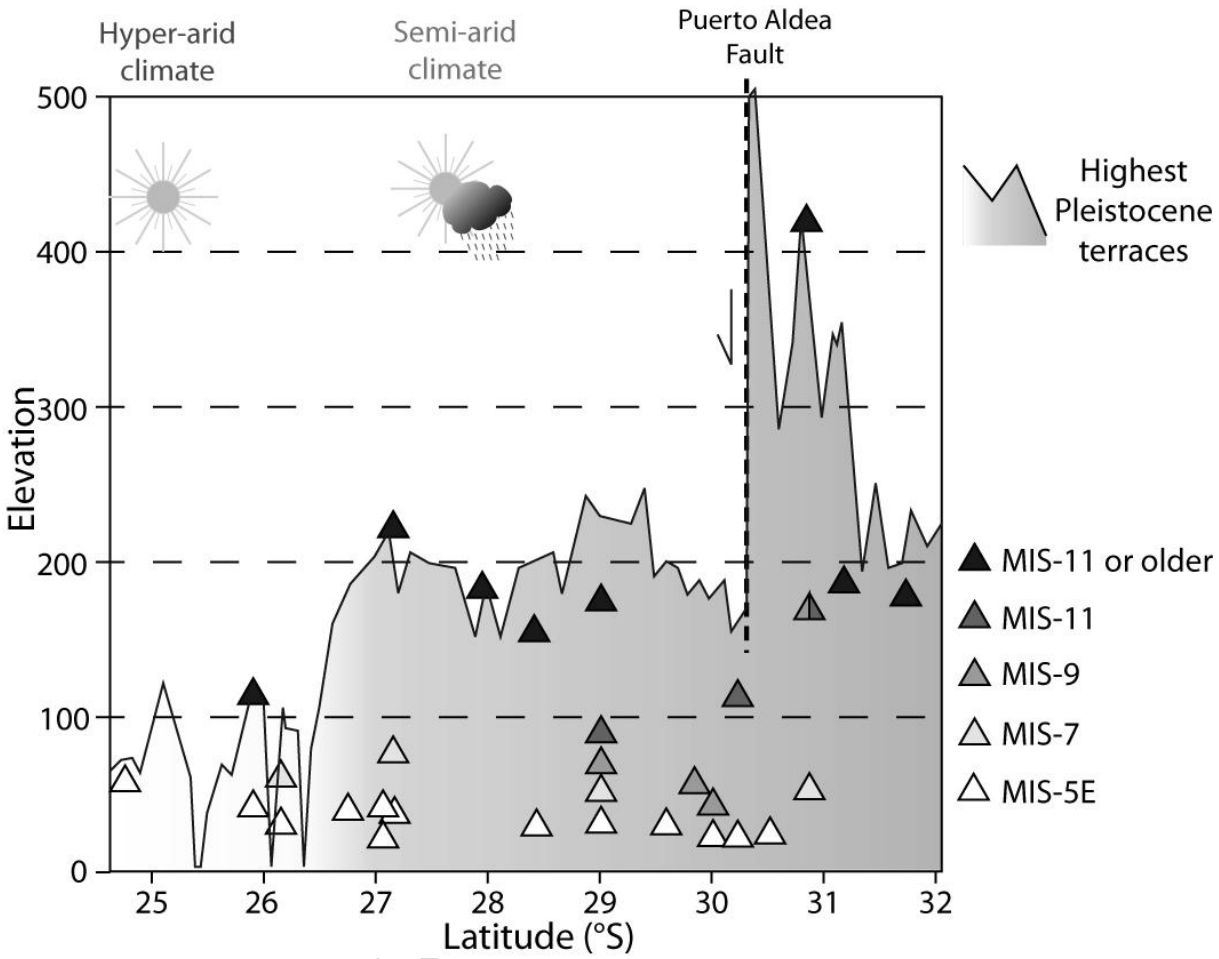

Figure 8: *Elevation of dated terraces along the coasts of Norte Chico. We also report the elevation of the highest preserved Pleistocene terrace vs. latitude.*

Fig. 8 presents the elevation of dated paleoshorelines between 24°S and 32°S. Despite most segments of the Norte Chico coasts have been uplifting at rates approaching 0.3 mm/yr since MIS-11, the higher elevation of Pleistocene paleoshorelines generally does not exceed 250 m amsl (Fig. 8), except in the Altos de Talinay area where terraces higher than 400 m amsl are observed. Older Neogene marine deposits, although locally present along the coast (Fig. 1), generally outcrop at smaller elevations than the higher Pleistocene paleoshorelines. It means that coastal uplift in the study area is recent, possibly younger than 1 Myr, or at least that it accelerated significantly during the Pleistocene (Regard et al., 2010). The morphology of marine terraces also suggests that the Middle and Upper Pleistocene uplift followed a period of stability of the continent, the higher terrace

being generally much wider and smoother than lower ones (Fig. 3). The same conclusion has been proposed by Rodriguez et al. (2013). These authors studied the morphology of the Choapa River valley that flows to the Pacific Ocean close to Chigualoco (31.6°S), and its connection with the coastal morphology. They observe that this valley is marked by a large upper fluvial terrace that penetrates more than 25 km inland, incised by a narrow valley in which the river flows to the ocean. The large fluvial terrace connects with the upper marine surface, suggesting that both formed during a period of relative stability of the coastal area with respect to sea level.

Along the coasts of Northern Chile, stability and/or subsidence prevailed during the Miocene, which contrasts with the present-day uplift (Fuenzalida et al., 1965; Paskoff, 1978; Le Roux et al., 2005; Clift & Hartley, 2007). Thus, external forearc vertical motions in Northern Chile obey a temporal scenario completely distinct from that prevailing in the high Cordillera, where a major uplift episode is believed to have occurred in the Miocene (e.g., Gregory-Wodzicki, 2000; Farias et al., 2005; Garzione et al., 2006; Aguilar et al., 2011). The possible causes of the Pleistocene accelerated coastal uplift are beyond the scope of this paper, but since it affects a coastal segment whose length is almost 1000 km, local causes such as seamount subduction or local tectonics cannot explain its onset. In fact, models show that several parameters related to plate dynamics, such as the convergence velocity or the interplate stresses, may result in forearc uplift or subsidence (Pedoja et al., 2011; Martinod et al., 2016). Higher Pleistocene paleoshorelines observed between 30.3°S and 31.3°S (Altos de Talinay area), in contrast, correspond to a local anomaly resulting from the activity of the Puerto Aldea Fault and other N-S oriented faults that accommodated the relative uplift of their western (coastal) block.

5.3. Different coastal morphology north and south 26.75°S: role of climate and marine erosion

Elsewhere than in the Altos de Talinay area, the elevation of the higher paleoshoreline is generally approximately 200 m amsl between 32°S and 27°S. North of 26.75°S, the width of the coastal fringe

narrows, the higher preserved paleoshorelines are generally below 100 m amsl (Fig. 8), and in few places, they are totally absent. This contrast is not explained by the present-day uplift rates, since most of the coasts have been uplifting at similar velocities during the Upper Pleistocene (and northern segments apparently somewhat quicker than southern segments of the coast). A younger initiation of coastal uplift north of 26.75°S may explain the absence of high Pleistocene paleoshorelines in the northern part of the study area. Nevertheless, this does not explain why MIS-5 terraces in the north are much more discreet and narrow than in the south. Everywhere in the study area, the coastal lithology is dominated by Mesozoic igneous rocks (Fig. 1). Hence, lithology does not explain the different morphology north of 26.75°S.

In fact, 26.75°S marks a major change in the morphology of both the coastal area and Coastal Cordillera. South of 26.75°S, the climate of northern Chile is semi-arid (Fig. 1), and rivers flow from the Western Cordillera through the Coastal Cordillera to the ocean. 26.75°S corresponds to the southern boundary of the hyper-arid Atacama Desert. In Chile, it is known as the boundary between the semi-arid Norte Chico, and the hyper-arid Norte Grande area, in which Quaternary erosion of the Coastal Cordillera by rivers has been particularly small. North of 26.75°S, the elevation of the coastal scarp suddenly increases. The coastal scarp is a major morphological feature of Northern Chile whose average elevation approaches 1000 m. Its occurrence is related to the hyper-arid climate of that part of the coast (Paskoff, 1978; Quezada et al., 2010). Continental erosion prevailing south of 26.75°S does not allow the preservation of such a high scarp and results in a lower continent close to the coast.

The widening of marine terraces by marine erosion during sea-level highstands requires the attack of the base of the scarp by the mechanical action of waves, and the collapse of the cliff. Debris fallen at the base of the cliff protect it from further erosion until they are evacuated by the ocean. Therefore, higher scarps should retreat more slowly, as observed in analogue experiments by Damgaard & Dong (2004) or Caplain et al. (2011). In the coastal segment located north of Tal-Tal

(25.4°S), the fringe located between the base of the coastal scarp and the ocean, is often covered by thick caps of fallen debris. In many places, the bedrock is not visible at the scarp toe and the ocean is actively eroding the cap of fallen debris. It suggests that the process limiting the widening of the terrace may not be erosion of the bedrock by waves but the time necessary to evacuate fallen debris, because the volume of debris is much larger for a similar coastal retreat when the scarp is higher (Fig. 9). This may explain why, despite comparable uplift rates, marine terraces are particularly narrow and poorly preserved in the northern part of the study area. Narrow terraces are easily erased by marine erosion during the following highstand period. The same result is obtained by Melnick (2016) in numerical models reproducing the appearance of coastal staircase sequences in uplifting continents. Models show that for comparable uplift rates, high terraces are preserved if the initial continental slope is small, whereas they are eroded and disappear beneath the coastal scarp when the continental slope is large.

Then, the presence of the high coastal scarp and the absence of widely preserved paleoshorelines may not necessarily imply that the coast has not been uplifting during the Pleistocene. We propose instead that the present-day morphological segmentation of the coast at 26.75°S marks the transition from the semi-arid Norte Chico to the hyper-arid Norte Grande climate, rather than latitudinal changes in the Pleistocene uplift velocities.

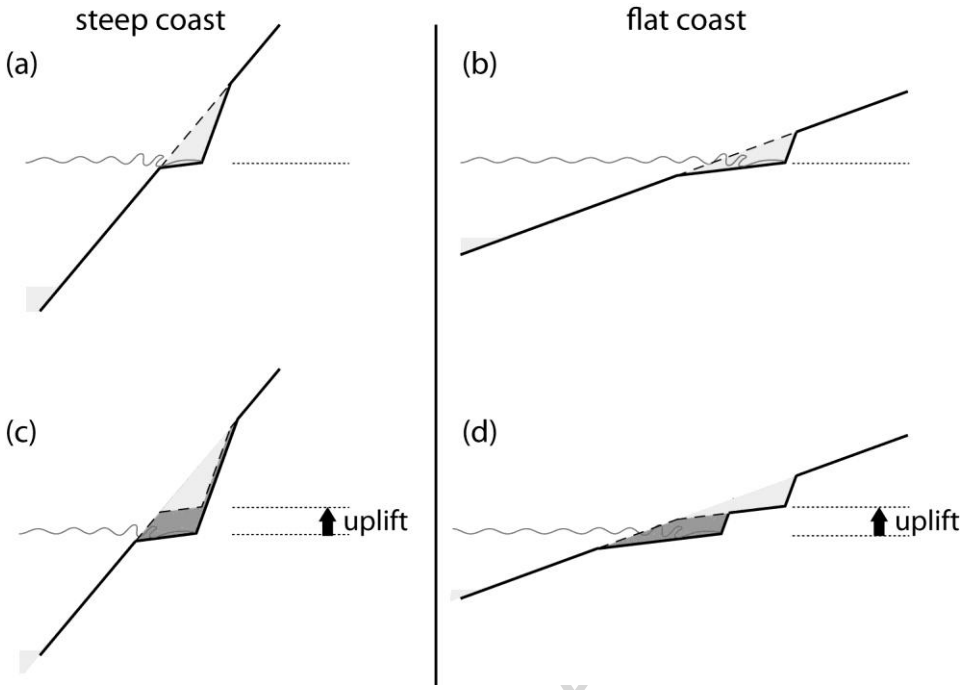

Figure 9: *Simple sketch of marine erosion, supposing that the evacuation of debris fallen at the base of the cliff is the process that limits the retreat of the cliff. (a) If the coast is steep, cliff retreat is small. The dashed and thick solid line represents the topographic profile before and after the highstand period, respectively. (b) The shore platform is larger in flat coasts, for a similar volume of evacuated debris (light gray area). During the next highstand sea level, the coast has been uplifted. (c) The narrow platform formed during the first highstand period in the steep coast is rapidly eroded, and marine erosion further attacks the old cliff. (d) In flat coast, for a similar volume of evacuated debris (dark gray area), marine erosion does not erase the ancient platform.*

6. Conclusions

Cosmogenic (^{10}Be) concentrations were measured in Pleistocene marine terraces of northern Chile between 24°S and 32°S show that onshore erosion rates following the emergence of paleoshorelines approached 1 m/Myr. Then, minimum ages calculated without erosion may be largely underestimated for Middle Pleistocene terraces, and it is not possible to assign paleoshorelines to particular sea-level highstands for these terraces. The analysis of both new cosmogenic data and

previously published ages shows that the Upper Pleistocene uplift rate has been 0.28 +/- 0.15 mm/yr in the study area. Data do not show major changes in uplift rate between neighboring points, suggesting that this uplift is a regional phenomenon related to the dynamics of the entire forearc area. Active faulting does not seem to affect coastal uplift, except in the Altos de Talinay area during the Middle Pleistocene. Since the maximum elevation of Pleistocene paleoshorelines in Northern Chile is generally close to 250 m amsl, measured rates imply that coastal uplift accelerated during the Pleistocene following a period of stability of the forearc, as already proposed by Regard et al. (2010) and Rodriguez et al. (2013). Data confirm, however, that the coastal uplift rate has been rather constant during the Middle and Upper Pleistocene in most of the study area (Fig. 7), as already observed in Bahia Inglesa by Quezada et al. (2010). Within this period, brief pulses of very rapid uplift are not apparent, except possibly in Altos de Talinay where an episode of rapid uplift may have occurred during the Middle Pleistocene when crustal faulting was active. However, considering dating uncertainties resulting from post-emergence erosion implies that maximum uplift rates may have been lower than proposed by Saillard et al. (2009). Although Pleistocene uplift rates are comparable everywhere in the study area, we observe that the morphology of the coast largely depends on the onshore continental slope. North of 26.75°S, the presence of a coastal scarp (whose preservation is encouraged by the hyper-arid climate of the Atacama Desert) inhibits the growth of marine terraces. This particular morphology of the coast may explain why paleoshorelines are poorly preserved between 26.75°S and 24°S despite Upper Pleistocene uplift rates being comparable with those prevailing in the southern part of the study area.

Acknowledgments: This work has been financed by the Institut National des Sciences de l'Univers, France (Syster program), by the International Mixt Laboratory "Copedim", and by the ECOS-Conicyt program (project C11U02). Authors thank editor (A.J. Plater), D. Melnick and an anonymous reviewer for their detailed and constructive comments which helped us to largely improve the manuscript.

References

Aguilar, G., Riquelme, R., Martinod, J., Darrozes, J., Maire, E., 2011. Variability in erosion rates related to the state of landscape transience in the semi-arid Chilean Andes. Earth Surf. Process. Landf. 36, 1736–1748.

Balco, G., Stone, J.O., Lifton, N.A., Dunai, T.J., 2008. A complete and easily accessible means of calculating surface exposure ages or erosion rates from (10)Be and (26)Al measurements. Quat. Geochronol. 3, 174–195.

Braucher, R., Brown, E.T., Bourles, D.L., Colin, F., 2003. In situ produced Be-10 measurements at great depths: implications for production rates by fast muons. Earth Planet. Sci. Lett. 211, 251–258.

Braucher, R., Merchel, S., Borgomano, J., Bourles, D.L., 2011. Production of cosmogenic radionuclides at great depth: A multi element approach. Earth Planet. Sci. Lett. 309, 1–9.

Brüggen, J.M., 1929. Texto de geología. El globo Ed., Santiago, Chile, 460 pp.

Brüggen, J.M., 1950. Fundamentos de la geología de Chile. Instituto Geográfico Militar Ed., Santiago, Chile, 374 pp.

Caputo, R., 2007. Sea-level curves: Perplexities of an end-user in morphotectonic applications. Glob. Planet. Change 57, 417–423.

Caplain, B., Astruc, D., Regard, V., Moulin, F.Y., 2011. Cliff retreat and sea bed morphology under monochromatic wave forcing: Experimental study. C. R. Geosci. 343, 471–477.

Chappell, J., 1974. Geology of Coral Terraces, Huon-Peninsula, New-Guinea - Study of Quaternary Tectonic Movements and Sea-Level Changes. Geol. Soc. Am. Bull. 85, 553–570.

Clift, P.D., Hartley, A.J., 2007. Slow rates of subduction erosion and coastal underplating along the Andean margin of Chile and Peru. Geology 35, 503–506.

Cooke, R.U, 1964. Les niveaux marins des baies de La Serena et de l'Huasco dans le nord du Chili. Bulletin de l'Association de géographes français 320, 19–32.

Cortes, J., 2012. Upper-plate fault activity in the Coastal Forearc of nothern Chile (~23°30'S): Paleoseismology, neotectonic implications and relation with the subduction cycle. Ph.D Thesis, Université Paul Sabatier (Toulouse, France) and Universidad Católica del Norte (Antofagasta, Chile).

Damgaard, J.S., Dong, P., 2004. Soft cliff recession under oblique waves: Physical model tests. J. Waterw. Port Coast. Ocean Eng.-ASCE 130, 234–242.

Darwin, C.R., 1846. Voyage of a naturalist, or journal of researches into the natural history and geology of the countries visited during the voyage of H. M. S. Beagle round the world, under the command of Capt. Fitz Roy. Harper and Brothers Ed., New York, United States.

Domeyko, I., 1848. Mémoire sur le terrain tertiaire et les lignes d'ancien niveau de l'Océan du sud, aux environs de Coquimbo (Chili). Annales des Mines 14, 153–162.

Farias, M., Charrier, R., Comte, D., Martinod, J., Hérail, G., 2005. Late Cenozoic deformation and uplift of the western flank of the Altiplano: Evidence from the depositional, tectonic, and geomorphologic evolution and shallow seismic activity (northern Chile, 19°30'S). Tectonics 24. doi:10.1029/2004TC001667 (TC4001).

Fuenzalida, H., Cooke, R., Paskoff, R., Segerstrom, K., Weischet, W., 1965. High Stands of Quaternary Sea Level Along the Chilean Coast. Geological Society of America Special Papers, 84, 473–496.

Garzione, C.N., Molnar, P., Libarkin, J.C., MacFadden, B.J., 2006. Rapid late Miocene rise of the Bolivian Altiplano: Evidence for removal of mantle lithosphere. Earth Planet. Sci. Lett. 241, 543–556.

Gregory-Wodzicki, K.M., 2000. Uplift history of the Central and Northern Andes: A review. Geol. Soc. Am. Bull. 112, 1091–1105.

Guilcher, A., 1974. Les «□ rasas□ »□ : Un problème de morphologie littorale généraleAnnales de Géographie 83, 1–33.

Henry, H., Regard, V., Pedoja, K., Husson, L., Martinod, J., Witt, C., Heuret, A., 2014. Upper Pleistocene uplifted shorelines as tracers of (local rather than global) subduction dynamics. J. Geodyn. 78, 8–20.

Jara-Munoz, J., Melnick, D., 2015. Unraveling sea-level variations and tectonic uplift in wave-built marine terraces, Santa Maria Island, Chile. Quat. Res. 83, 216–228.

Jara-Munoz, J., Melnick, D., Strecker, M.R., 2016. TerraceM: A MATLAB (R) tool to analyze marine and lacustrine terraces using high-resolution topography. Geosphere 12, 176–195.

Kober, F., Ivy-Ochs, S., Schlunegger, F., Baur, H., Kubik, P.W., Wieler, R., 2007. Denudation rates and a topography-driven rainfall threshold in northern Chile: Multiple cosmogenic nuclide data and sediment yield budgets. Geomorphology 83, 97–120.

Lajoie, K.R., 1986. Costal tectonics. In: Active Tectonics. National Academy Press Ed., Washington D.C., pp. 95–124.

Le Roux, J.P., Gomez, C.A., Olivares, D.M., Middleton, H., 2005. Determining the Neogene behavior of the Nazca plate by geohistory analysis. Geology 33, 165–168.

Leonard, E., Wehmiller, J., 1992. Low Uplift Rates and Terrace Reoccupation Inferred from Mollusk Aminostratigraphy, Coquimbo Bay Area, Chile. Quat. Res. 38, 246–259.

Leonard, E.M., Muhs, D.R., Ludwig, K.R., Wehmiller, J.F., 1994. Coral Uranium-series ages and mollusc amino-acid ratios from uplifted marine terrace deposits, Morro de Copiapo, northcentral Chile. In: American Quaternary Association Program and Abstracts, 13th biennal meeting, pp. 223.

Marquardt, C., 1999. Neotectónica de la franja costera y aportes a la geología regional entre Caldera y Caleta Pajonal (27° - 27°45'S), tercera región de Atacama. Magister thesis, Universidad de Chile (Santiago, Chile).

Marquardt, C., Lavenu, A., Ortlieb, L., Godoy, E., Comte, D., 2004. Coastal neotectonics in Southern Central Andes: uplift and deformation of marine terraces in Northern Chile (27°S). Tectonophysics 394, 193–219.

Martinod, J., Regard, V., Letourmy, Y., Henry, H., Hassani, R., Baratchart, S., Carretier, S., 2016. How do subduction processes contribute to forearc Andean uplift? Insights from numerical models. Journal of Geodynamics 96, 6–18.

Melnick, D., 2016. Rise of the central Andean coast by earthquakes straddling the Moho. Nature Geosci, doi:10.1038/ngeo2683.

Nishiizumi, K., Caffee, M.W., Finkel, R.C., Brimhall, G., Mote, T., 2005. Remnants of a fossil alluvial fan landscape of Miocene age in the Atacama Desert of northern Chile using cosmogenic nuclide exposure age dating. Earth and Planetary Science Letters 237, 499–507.

Nishiizumi, K., Imamura, M., Caffee, M., Southon, J., Finkel, R., McAnich, J., 2007. Absolute calibration of Be-10 AMS standards. Nuclear Instruments and Methods: Physics Research 258, 403–413.

Ortlieb, L., Guzman, N., Marquardt, C., 2003. A Longer-Lasting and Warmer lnterglacial Episode During Isotopic Stage 11: Marine Terrace Evidence in Tropical Western Americas. In: Drowler, A.W., Poore, R.Z., Burkle, L.H. (Eds.), Earth Climate and Orbital Excentricity; the Marine Isotopic Stage 11 Question, Geophysical Monograph, Vol. 137, pp. 157–180.

Ota, Y., Miyauchi, T., Paskoff, R., Koba, M., 1995. Plioquaternary Marine Terraces and Their Deformation Along the Altos De Talinay, North-Central Chile. Rev. Geol. Chile 22, 89–102.

Paskoff, R., 1970. Recherches géomorphologiques dans le Chili semi-aride. Biscaye frères Ed., Bordeaux, France, 420 pp.

Paskoff, R.P., 1978. Sur l'évolution géomorphologique du grand escarpement côtier du désert chilien. Géographie Physique et Quaternaire 32, 351–360.

Pedoja, K., Husson, L., Regard, V., Cobbold, P.R., Ostanciaux, E., Johnson, M.E., Kershaw, S., Saillard, M., Martinod, J., Furgerot, L., Weill, P., Delcaillau, B., 2011. Relative sea-level fall since the last interglacial stage: Are coasts uplifting worldwide? Earth-Sci. Rev. 108, 1–15.

Pedoja, K., Husson, L., Johnson, M.E., Melnick, D., Witt, C., Pochat, S., Nexer, M., Delcaillau, B., Pinegina, T., Poprawski, Y., Authemayou, C., Elliot, M., Regard, V., Garestier, F., 2014. Coastal staircase sequences reflecting sea-level oscillations and tectonic uplift during the Quaternary and Neogene. Earth-Sci. Rev. 132, 13–38.

Quezada, J., Gonzalez, G., Dunai, T., Jensen, A., Juez-Larre, J., 2007. Pleistocene littoral uplift of northern Chile: Ne-21 age of the upper marine terrace of Caldera-Bahia Inglesa area. Rev. Geol. Chile 34, 81–96.

Quezada, J., Cerda, J.L., Jensen, A., 2010. Tectonic and climatic effects in the morphologic configuration of the coastal relief of northern Chile. Andean Geol. 37, 78–109.

Radtke, U., 1989. Marine Terrassen und Korallenriffe. Das problem der Quartären Meerespiegelschwankungen erlänter an Fallstudien aus Chile, Argentinien und Barbados. Düsseldorfer geographische Schriften, Vol.27 (246 pp.).

Radtke, U., 1987a. Marine terraces in Chile (22°-32°S), geomorphology, chronostratigraphy and neotectonics: preliminary results. In: INQUA international congress. 12, pp. 239–256.

Radtke, U., 1987b. Palaeo sea levels and discrimination of the last and the penultimate interglacial fossiliferous deposits by absolute dating methods and geomorphological investigations illustrated from marine terraces in Chile. Berliner Geographische Studien 25, 313–342.

Regalla, C., Fisher, D.M., Kirby, E., Furlong, K.P., 2013. Relationship between outer forearc subsidence and plate boundary kinematics along the Northeast Japan convergent margin. Geochemistry, Geophysics, Geosystems 14, 5227-5243.

Regard, V., Saillard, M., Martinod, J., Audin, L., Carretier, S., Pedoja, K., Riquelme, R., Paredes, P., Hérail, G., 2010. Renewed uplift of the Central Andes Forearc revealed by coastal evolution during the Quaternary. Earth Planet. Sci. Lett. 297, 199–210.

Rodriguez, M.P., Carretier, S., Charrier, R., Saillard, M., Regard, V., Hérail, G., Hall, S., Farber, D., Audin, L., 2013. Geochronology of pediments and marine terraces in north-central Chile and their implications for Quaternary uplift in the Western Andes. Geomorphology 180, 33–46.

Saillard, M., Hall, S.R., Audin, L., Farber, D.L., Hérail, G., Martinod, J., Regard, V., Finkel, R.C., Bondoux, F., 2009. Non-steady long-term uplift rates and Pleistocene marine terrace development along the Andean margin of Chile (31°S) inferred from Be-10 dating. Earth Planet. Sci. Lett. 277, 50–63.

Saillard, M., Hall, S.R., Audin, L., Farber, D.L., Martinod, J., Regard, V., Pedoja, K., Hérail, G., 2010. Reply to a Comment on "Non-steady long-term uplift rates and Pleistocene marine terrace development along the Andean margin of Chile (31°S) inferred from Be-10 dating" Earth Planet. Sci. Lett. 296, 506–509.

Saillard, M., Hall, S.R., Audin, L., Farber, D.L., Regard, V., Hérail, G., 2011. Andean coastal uplift and active tectonics in southern Peru: Be-10 surface exposure dating of differentially uplifted marine terrace sequences (San Juan de Marcona, ~15.4°S). Geomorphology 128, 178–190.

Saillard, M., Riotte, J., Regard, V., Violette, A., Hérail, G., Audin, L., Riquelme, R., 2012. Beach ridges U-Th dating in Tongoy bay and tectonic implications for a peninsula-bay system, Chile. J. South Am. Earth Sci. 40, 77–84.

Siddall, M., Chappell, J., Potter, E.K., 2006. Eustatic sea level during past interglacials. In: Sirocko, F., Claussen, M., Sanchez Goñi, M.F., Litt, T. (Eds.), The Climate of Past Interglacials. Elsevier, Amsterdam, pp. 75–92

Simms, A.R., Rouby, H., Lambeck, K., 2016. Marine terraces and rates of vertical tectonic motion: The importance of glacio-isostatic adjustment along the Pacific coast of central North America. Geol. Soc. Am. Bull. 128, 81–93.

Willmott, C. J., Matsuura, K., 2001. Terrestrial Air Temperature and Precipitation: Monthly and Annual Time Series (1950 - 1999). http://climate.geog.udel.edu/~climate/html_pages/README.ghcn_ts2.html

Figure Captions

Figure 1: (a) Location of dated marine paleoshorelines and other sites cited in the text. Empty triangles: ^{10}Be data on surface samples; filled triangles: ^{10}Be data in vertical profiles; diamonds: other dating methods; (b) Basement lithology along the coast; (c) Average annual precipitations between 1960 and 1990 (after Willmott & Matsuura, 2001); (d) Topographic profiles perpendicular to the coast.

Figure 2: View from the South of the Punta Piedras terrace beneath the coastal scarp (24.75°S).

Figure 3: Contrasted morphology of the upper and lower terraces in Punta Tetillas (29°S). (a) The upper terrace is several km wide, and it has been almost completely polished by marine erosion. Only rare seastacks have been preserved. (b) View taken from the upper surface towards the

ocean and (c) photo taken from one of the lower terraces. Lower terraces are rough, narrow, and shoreline angles marking different highstand levels may be difficult to observe.

Figure 4: Latitude vs. elevation of dated paleoshorelines. Circles correspond to paleoshorelines dated in previous studies, filled circles corresponding to paleoshorelines dated using cosmogenic isotopes whose ages are discussed again in this paper. Triangles correspond to paleoshorelines sampled and dated in this work.

Figure 5: ^{10}Be concentrations along vertical profiles sampled in marine terraces in Chigualoco and Huasco. The solid and dashed lines in the Chigualoco profile represent the best fit obtained using the cosmogenic production rates proposed by Balco et al. (2008) and by Braucher et al. (2011), respectively.

Figure 6: Map and inner edge elevation of coastal terraces located close to Caleta Chañaral. The location of detailed maps (c) and (d) is given in (a). (b) Assigning terraces to successive odd-numbered isotopic stages (colored triangles) implies a remarkably constant uplift rate close to 0.25 mm/yr. Minimum ages deduced from ^{10}Be concentrations in samples from Punta Tetillas (empty diamonds) confirm that T1 corresponds to MIS-5, and that the higher 160 m amsl terrace is older than 600 kyrs. See the text for the discussion of ^{10}Be concentrations.

Figure 7: Absolute uplift rates calculated considering Pleistocene eustatic variations proposed by Siddall et al. (2006) (see Table 3)

Figure 8: Elevation of dated terraces along the coasts of Norte Chico. We also report the elevation of the highest preserved Pleistocene terrace vs. latitude.

Figure 9: Simple sketch of marine erosion, supposing that the evacuation of debris fallen at the base of the cliff is the process that limits the retreat of the cliff. (a) If the coast is steep, cliff retreat is small. The dashed and thick solid line represents the topographic profile before and after the highstand period, respectively. (b) The shore platform is larger in flat coasts, for a similar volume of evacuated debris (light gray area). During the next highstand sea level, the coast has been uplifted. (c) The narrow platform formed during the first highstand period in the steep coast is

rapidly eroded, and marine erosion further attacks the old cliff. (d) In flat coast, for a similar volume of evacuated debris (dark gray area), marine erosion does not erase the ancient platform.

Table 1: ^{10}Be concentrations in samples collected along the coasts of Chile between 24°S and 32°S. [1] new data; [2] data published in Saillard et al. (2009); [3] data published in Rodriguez et al. (2013).

Table 2: ^{10}Be concentrations measured in surface samples, and corresponding ages calculated considering different erosion rates between 0 and 1.5 m/Myr using the Cronus-Earth web calculator (Balco et al., 2008)

Table 3: Correlation of dated terraces to MIS, corresponding apparent and absolute uplift rates. Minimum and maximum absolute uplift rates have been calculated considering uncertainties on sea-level highstand elevations and ages proposed by Siddall et al. (2006) (Table 4), and an uncertainty of $\pm$ 5 m in the elevation of shoreline angles. [1] new data published in this paper; Data after [2] Rodriguez et al. (2013); [3] Saillard et al. (2009); [4] Radtke (1987b); [5] Radtke (1987a); [6] Radtke (1989); [7] Saillard et al. (2012); [8] Leonard & Wehmiller (1992) ; [9] Marquardt et al. (2004) ; [10] Quezada et al. (2007). MIS correlations proposed by Rodriguez et al. (2013) and Saillard et al. (2009) are discussed in section 5.1.

Table 4: Age of Middle and Upper Pleistocene highstands and corresponding sea-level elevations (after Siddall et al., 2006), adopted to estimate the absolute uplift rates presented in Table 3.

Sample name	Latitude (°S)	Longitude (°W)	Elevation (m asl)	Ref.	Sample	Mass dissolved quartz (g)	Spike ^{9}Be (at)	+/-	Corrected ^{10}Be/ ^{9}Be (x 10^{-15})	+/-	depth (m)	^{10}Be (at/g)	+/-
Chigualoco-1	31,7008	71,5181	146	[1]	altered bedrock	9,4663	503,57	16,18	1083564	34967	0,3	1083564	34967
Chigualoco-2	31,7008	71,5181	146	[1]	altered bedrock	8,5798	379,81	14,83	902877	35350	0,5	902877	35350
Chigualoco-3	31,7008	71,5181	146	[1]	altered bedrock	16,173	505,90	18,68	638487	23655	0,65	638487	23655
Chigualoco-5	31,7008	71,5181	146	[1]	altered bedrock	26,5112	570,32	21,19	438672	16355	1,2	438672	16355
Chigualoco-6	31,7008	71,5181	146	[1]	altered bedrock	23,5001	320,38	12,30	277646	10691	2,15	277646	10691
Caleta Maiten	31,1517	71,6610	120	[2]	bedrock	--	--	--	--	--	0	1905192	34348
Caleta Maiten	31,1517	71,6610	121	[2]	cobble	--	--	--	--	--	0	1992154	43215
Caleta Maiten	31,1517	71,6610	120	[2]	cobble	--	--	--	--	--	0	2744604	48954
Altos de Talinay T1	30,9000	71,6600	241	[3]	bedrock	--	--	--	--	--	0	2940000	47400
Altos de Talinay T1	30,9000	71,6600	241	[3]	bedrock	--	--	--	--	--	0	2870000	51150
Altos de Talinay T1	30,9000	71,6600	241	[3]	bedrock	--	--	--	--	--	0	2910000	67800
Altos de Talinay T3	30,8700	71,6800	30	[3]	bedrock	--	--	--	--	--	0	913000	29600
Altos de Talinay T3	30,8700	71,6800	30	[3]	bedrock	--	--	--	--	--	0	833000	33300
Altos de Talinay T3	30,8700	71,6800	30	[3]	bedrock	--	--	--	--	--	0	937000	20500
Altos de Talinay T2	30,8400	71,6900	102	[3]	bedrock	--	--	--	--	--	0	1320000	38800
Altos de Talinay T2	30,8400	71,6900	102	[3]	bedrock	--	--	--	--	--	0	1313000	26600
Altos de Talinay T4	30,4800	71,6900	18	[3]	clasts	--	--	--	--	--	0	679000	16600
Altos de Talinay T4	30,4800	71,6900	18	[3]	clasts	--	--	--	--	--	0	620000	12000
Altos de Talinay T4	30,4800	71,6900	18	[3]	clasts	--	--	--	--	--	0	490000	9800
Caleta Chañaral 1	29,0199	71,4850	156	[1]	rounded pebbles	22,9412	1632,96	46,28	1438813	40780	0	1438813	40780
Caleta Chañaral 2	29,0199	71,4850	156	[1]	quartz clasts	23,5906	1975,23	55,70	1695867	47823	0	1695867	47823
Caleta Chañaral 3	29,0199	71,4850	156	[1]	bedrock	24,577	2933,29	78,95	2419287	65115	0	2419287	65115
Caleta Chañaral 4	29,0178	71,4791	164	[1]	rounded pebbles	22,3073	2137,55	73,60	1940815	66827	0	1940815	66827
Caleta Chañaral 5	29,0178	71,4791	164	[1]	quartz clasts	22,8192	2315,43	57,73	2053931	51209	0	2053931	51209
Caleta Chañaral 6	29,0178	71,4791	164	[1]	bedrock	22,5767	1944,33	56,06	1742916	50256	0	1742916	50256
Caleta Chañaral 7	29,0281	71,4856	88	[1]	bedrock	15,3402	549,86	18,84	734181	25249	0	734181	25249
Caleta Chañaral 8	29,0277	71,4851	91	[1]	bedrock	13,1428	399,20	12,52	625576	19713	0	625576	19713
Caleta Chañaral 9	29,0289	71,4954	30	[1]	bedrock	12,5605	352,31	16,65	573107	27130	0	573107	27130
Caleta Chañaral 10	29,0292	71,4958	28	[1]	bedrock	15,1905	427,94	23,32	573273	31280	0	573273	31280
Huasco-1	28,3878	71,1662	115	[1]	bedrock	23,3222	111,09	7,00	96624	6096	2,5	96624	6096
Huasco-2	28,3878	71,1662	115	[1]	bedrock	21,8183	--	--	--	--	1,7	--	--
Huasco-3	28,3878	71,1662	115	[1]	bedrock	22,704	274,74	23,82	246493	21380	1,4	246493	21380
Huasco-4	28,3878	71,1662	115	[1]	bedrock	21,9596	--	--	--	--	1,0	--	--
Huasco-5	28,3878	71,1662	115	[1]	bedrock	21,8483	1335,93	97,82	1241918	91012	0,25	1241918	91012
Caleta Sal 1	27,9336	71,1149	170	[1]	bedrock	23,6249	2171,25	70,25	1865179	60605	0	1865179	60605
Caleta Sal 2	27,9336	71,1149	170	[1]	rounded pebbles	22,4005	1429,98	47,98	1296315	43668	0	1296315	43668
Caleta Sal 3	27,9298	71,1108	158	[1]	bedrock	21,8393	1951,73	61,04	1810252	56869	0	1810252	56869
Pan de Azucar 1	26,1438	70,6476	64	[1]	bedrock	23,417	897,56	30,13	779663	26277	0	779663	26277
Pan de Azucar 2	26,1438	70,6484	53	[1]	bedrock	22,3457	1135,99	66,02	1034188	60183	0	1034188	60183
Pan de Azucar 3	26,1439	70,6484	60	[1]	bedrock	22,1231	838,44	59,49	770294	54702	0	770294	54702
Pan de Azucar 4	26,1439	70,6484	60	[1]	quartz clasts	21,9009	760,34	68,97	706748	64141	0	706748	64141
Esmeralda 1	25,9084	70,6711	115	[1]	quartz clasts	21,6562	1756,70	54,37	1655757	51484	0	1655757	51484
Esmeralda 4	25,9129	70,6717	45	[1]	bedrock	21,6161	339,28	24,34	318565	22871	0	318565	22871
Esmeralda 5	25,9133	70,6717	45	[1]	bedrock	21,9545	411,57	15,65	379655	14478	0	379655	14478
Esmeralda 6	25,9142	70,6717	45	[1]	bedrock	23,5633	350,18	16,73	301781	14442	0	301781	14442
Punta Piedras 1	24,7599	70,5509	61	[1]	bedrock	18,1454	543,85	17,98	606628	20055	0	606628	20055
Punta Piedras 2	24,7599	70,5511	61	[1]	bedrock	15,9007	386,10	13,21	491217	16806	0	491217	16806
Punta Piedras 3	24,7602	70,5520	60	[1]	bedrock	1,0794	25,51	2,53	478848	47528	0	478848	47528
Punta Piedras 4	24,7601	70,5515	59	[1]	clasts	22,67	667,62	21,11	595903	18845	0	595903	18845

AMS Standard: NIST 4325, using an assigned value of of (2.79±0.03).10E-11 (Nichiizumi 2007).

Table 1: *^{10}Be concentrations in samples collected along the coasts of Chile between 24°S and 32°S. [1] new data; [2] data published in Saillard et al. (2009); [3] data published in Rodriguez et al. (2013).*

Sample	Lat. (°S)	Long. (°W)	Elev.	10Be (at/g)	+/-	age e=0	+/-	age e=0,5	age e=1	age e=1,5	MIS
Caleta Maiten	-31.15	-71.66	120	1905000	34300	446512	44375	560198	827611	-	> 13
Caleta Maiten	-31.15	-71.66	121	1992000	43200	469064	47324	597697	932005	-	
Caleta Maiten	-31.15	-71.66	120	2745000	49000	680228	71839	1040360	-	-	
Altos de Talinay T1	-30.90	-71.66	241	2940000	47400	661875	69303	994299	-	-	> 15
Altos de Talinay T1	-30.90	-71.66	241	2870000	51150	643284	67275	948265	-	-	
Altos de Talinay T1	-30.90	-71.66	241	2910000	67800	653886	69550	974247	-	-	
Altos de Talinay T2	-30.84	-71.69	102	1320000	38800	304643	30174	350583	422065	559359	9-11
Altos de Talinay T2	-30.84	-71.69	102	1313000	26600	302899	29168	348242	418536	552410	
Altos de Talinay T3	-30.87	-71.68	30	913000	29600	218730	21429	240677	269741	310950	7
Altos de Talinay T3	-30.87	-71.68	30	833000	33300	198579	19962	216374	239192	270006	
Altos de Talinay T3	-30.87	-71.68	30	937000	20500	224815	21312	248118	279288	324191	
Altos de Talinay T4	-30.48	-71.69	18	679000	16600	162890	15313	174522	188665	206389	5
Altos de Talinay T4	-30.48	-71.69	18	620000	12000	148198	13689	157718	169057	182887	
Altos de Talinay T4	-30.48	-71.69	18	490000	9800	116202	10664	121914	128436	135979	
Caleta Chañaral 1	-29.02	-71.49	156	1438800	40800	330138	32796	385352	476266	677391	> 13
Caleta Chañaral 2	-29.02	-71.49	156	1695900	47800	395326	39914	479682	644968	1415992	
Caleta Chañaral 3	-29.02	-71.49	156	2419300	65100	591033	62524	828303	4222362	-	
Caleta Chañaral 4	-29.02	-71.48	164	1940800	66800	456292	47884	576176	869481	-	
Caleta Chañaral 5	-29.02	-71.48	164	2053900	51200	486384	49755	627300	1026436	-	
Caleta Chañaral 6	-29.02	-71.48	164	1742900	50300	404704	41054	493977	674180	1757996	
Caleta Chañaral 7	-29.03	-71.49	88	734200	25200	170837	16656	183718	199560	219726	-
Caleta Chañaral 8	-29.03	-71.49	91	625600	19700	144276	13822	153275	163938	176858	
Caleta Chañaral 9	-29.03	-71.49	30	573100	27100	138550	14188	146802	156501	168131	5
Caleta Chañaral 10	-29.03	-71.49	28	573300	31300	138831	14749	147118	156861	168550	
Caleta Sal 1	-27.93	-71.11	170	1865200	60600	444606	46171	556848	817768	-	> 9
Caleta Sal 2	-27.93	-71.11	170	1296300	43700	298238	29965	341962	409027	533720	
Caleta Sal 3	-27.93	-71.11	158	1810300	56900	434426	44818	540386	777004	-	
Pan de Azucar 1	-26.14	-70.65	64	780000	26300	195741	19160	212933	234854	264205	7
Pan de Azucar 2	-26.14	-70.65	53	1034200	60200	266281	29780	300012	348451	427244	
Pan de Azucar 3	-26.14	-70.65	60	770300	54700	193804	22831	210630	232020	260536	
Pan de Azucar 4	-26.14	-70.65	60	706700	64100	177072	23251	190933	208118	230232	
Esmeralda 4	-25.91	-70.67	45	318600	22900	79110	9098	81679	84479	87549	5
Esmeralda 5	-25.91	-70.67	45	379700	14400	94646	9186	98364	102494	107117	
Esmeralda 6	-25.91	-70.67	45	301800	14400	74860	7559	77153	79640	82351	
Esmeralda 1	-25.91	-70.67	115	1655800	51500	424300	43606	523938	737124	3400817	> 9
Punta Piedras 1	-24.76	-70.55	61	606600	20100	154473	14930	164824	177247	192547	5
Punta Piedras 2	-24.76	-70.55	61	491200	16800	124153	11957	130687	138217	147027	
Punta Piedras 3	-24.76	-70.55	60	478900	47500	121041	16451	127237	134349	142629	
Punta Piedras 4	-24.76	-70.55	60	596000	18800	151786	14572	161760	173684	188300	

Table 2: *^{10}Be concentrations measured in surface samples, and corresponding ages calculated considering different erosion rates between 0 and 1.5 m/Myr using the Cronus-Earth web calculator (Balco et al., 2008)*

Site	Latitude (°S)	Terrace shoreline angle Elevation (m)	MIS	Apparent uplift rate (mm/yr)	Minimum absolute uplift rate	Maximum absolute uplift rate	ref.
Punta Piedras	24.76	61	**5**	0.48	0.38	0.57	[1]
Esmeralda	25.91	115	**> 11**	< 0.27	-	0.27	[1]
Esmeralda	25.91	45	**5**	0.35	0.26	0.43	[1]
Pan de Azucar	26.14	33	**5**	0.25	0.17	0.33	[4]
Pan de Azucar	26.14	64	**7**	0.35	0.27	0.44	[1]
Caleta Obispito	26.75	43	**5**	0.33	0.24	0.41	[4]
Caldera	27.05	23	**5**	0.17	0.09	0.24	[4]
Caldera	27.05	44	**5**	0.34	0.25	0.42	[9]
Bahia Inglesa	27.15	40	**5**	0.31	0.22	0.39	[5] [9]
Bahia Inglesa	27.15	78	**7**	0.42	0.33	0.52	[4]
Bahia Inglesa	27.15	224	**> 13**	< 0.43	-	0.43	[10]
Caleta Sal	27.93	185	**> 9**	< 0.36	-	0.36	[1]
Huasco	28.39	155	**> 13**	< 0.30	-	0.30	[1]
Huasco	28.40	30	**5**	0.23	0.15	0.30	[4]
Caleta Chañaral	29.02	34	**5**	0.26	0.18	0.34	[1]
Caleta Chañaral	29.02	54	**7**	0.30	0.23	0.39	[1]
Caleta Chañaral	29.03	92	**11**	0.22	0.19	0.26	[1]
Caleta Chañaral	29.03	74	**9**	0.23	0.19	0.27	[1]
Caleta Chañaral	29.03	110	**13**	0.23	0.19	0.26	[1]
Caleta Chañaral	29.03	164	**> 13**	< 0.32	-	0.32	[1]
Quebrada Honda	29.60	33	**5**	0.25	0.17	0.33	[5]
Teatinos	29.82	58	**> 7**	< 0.17	-	0.17	[8]
Coquimbo	29.98	25	**5**	0.18	0.11	0.26	[6]
Coquimbo	29.98	41	**> 7**	< 0.20	-	0.12	[8]
Tongoy	30.20	25	**5**	0.18	0.11	0.26	[4] [7]
Tongoy	30.20	114	**11**	0.29	0.24	0.33	[7]
Altos de Talinay	30.48	25	**5**	0.18	0.11	0.26	[3]
Altos de Talinay	30.84	170	**9-11**	0.52-0.42	0.37	0.57	[3]
Altos de Talinay	30.87	55	**7**	0.31	0.23	0.39	[3]
Altos de Talinay	30.90	425	**> 15**	< 0.67	-	0.67	[3]
Caleta Maiten	31.15	185	**> 13**	< 0.36	-	0.36	[2]
Chigualoco	31.70	180	**> 11**	< 0.41	-	0.41	[1]

Table 3: *Correlation of dated terraces to MIS, corresponding apparent and absolute uplift rates. Minimum and maximum absolute uplift rates have been calculated considering uncertainties on sea-level highstand elevations and ages proposed by Siddall et al. (2006) (Table 4) , and an uncertainty of ± 5 m in the elevation of shoreline angles. [1] new data published in this paper; Data after [2] Rodriguez et al. (2013); [3] Saillard et al. (2009); [4] Radtke (1987b); [5] Radtke (1987a); [6] Radtke (1989); [7] Saillard et al. (2012); [8] Leonard & Wehmiller (1992) ; [9] Marquardt et al. (2004) ; [10]*

Quezada et al. (2007). MIS correlations proposed by Rodriguez et al. (2013) and Saillard et al. (2009) are discussed in section 5.1.

highstand	Sea level (m amsl)	Age (kyr)
MIS 5e	3 ± 3	116 - 131
MIS 7	-10 ± 5	190 - 235
MIS 9	2 ± 5	315 - 334
MIS 11	0 ± 10	395 - 415
MIS 13	0 ± 10	472 - 502
MIS 15	0 ± 10	558 - 620
MIS 17	-15 ± 15	685 - 695

Table 4: *Age of Middle and Upper Pleistocene highstands and corresponding sea-level elevations (after Siddall et al., 2006), adopted to estimate the absolute uplift rates presented in Table 3.*

Highlights:

- We date paleoshorelines in Chile between 24°S and 32°S using ^{10}Be concentrations data
- Post-emergence erosion of abrasion shore terraces approaches 1 m/Myr
- The coast has been uplifting at ~0.3 mm/yr during the Upper Pleistocene
- Uplift velocity increased during the Pleistocene following a period of stability
- Paleoshorelines are poorly preserved beneath the northern coastal scarp